JPRS-UCH-91-007
26 JULY 1991

JPRS Report

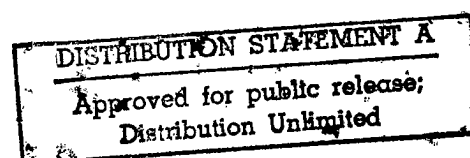# Science & Technology

USSR: Chemistry

DTIC QUALITY INSPECTED 2

19990305 048

Science & Technology
USSR: Chemistry

CONTENTS

CHEMICAL INDUSTRY

COMBUSTION, EXPLOSIVES

ELECTROCHEMISTRY

LASER MATERIALS

POLYMERS, RUBBER

RADIATION CHEMISTRY

MISCELLANEOUS

Preproduction Tests of Nonplatinum Ammonia Oxidation Catalysts

[Article by M.M. Karavayev, N.F. Kleshchev, N.P. Levshin, Yu.V. Semenov, and I.V. Nakaznaya]

UDC 661.53.094.373

[Abstract] The ammonia oxidation process used in the production of nonconcentrated nitric acid in the USSR requires the use of more than 7 tons of platinum alloys annually. The increasing scarcity and cost of platinum on the international market have made it necessary to find alternatives to the use of platinum alloys. Working together with T.Ye. Molchanova, N.B. Guba, and G.V. Mikisha, the authors of the study reported herein conducted a series of tests designed to determine the technological conditions and specifics of the use of a purely nonplatinum ammonia oxidation catalyst under commercial conditions. The tests were conducted in a specially created pilot contact device 1,000 mm in diameter. An ammonia-and-air mixture was fed from one of the commercial units. The nitroso gases formed were directed to a commercial waste-heat boiler, after which they were processed into nonconcentrated nitric acid. The contact device's piping circuit made it possible to vary the temperature of the ammonia-and-air mixture and the mixture's ammonia contact within a broad range. The gas mixtures were analyzed in accordance with methods described elsewhere. As their nonplatinum catalyst the researchers use a contact based on the system Co_3O_4, i.e., a heat-resistant oxide with two promoters that was conditionally called KN-K5. The total height of the layer was between 34 and 36 mm. The nonplatinum catalyst was fired by a nitrogen-and-hydrogen mixture by using a method that is described in detail elsewhere. A 3- to 4-mm layer of pure Co_3O_4 was poured on top of the nonplatinum catalyst layer to reduce the firing temperature. The nonplatinum catalyst was prepared on commercial equipment by decomposing nitrates. The maximum NO yield (on the order of 96%) was achieved when the ammonia-and-air mixture was heated to 350°C. Reducing the temperature to 240°C reduced the NO yield to 88%. The preproduction tests conducted confirmed that the KN-K5 nonplatinum ammonia oxidation catalyst can be used effectively for an extended period (more than 2,000 hours). Tests conducted for over 2,000 hours (with stops at 120, 240, and 1,075 hours) confirmed that the KN-K5 catalyst continues to oxidize ammonia with a rather high (up to 96%) yield of nitrogen (II) oxide. Furthermore, the catalyst's selectively did not change significantly over the entire test period. Although the safety of the process using the new nonplatinum catalyst was comparable to that of the process involving a platinum catalyst, the current method of heating nonplatinum catalysts is unsuitable for nonplatinum catalysts, and an alternative must be found. The authors state that main problem in the field of nonplatinum catalysts for the near future is to create specimens possessing a sharply increased activity when compared with the existing contacts or possessing high selectivity over a wide temperature range (500 to 900°C). Figures 4; references 8: 6 Russian, 2 Western.

Separating Krypton and Xenon From Ammonia Synthesis Blowdown Gases

[Article by S.A. Arutyunov (deceased), Ya.D. Zelvenskiy, V.A. Shitikov]

UDC 661.939:661.53.094.373

[Abstract] The process of separating krypton and xenon from oxygen is complex and involves many stages. This is due to the low concentrations in which krypton and xenon are found and to the fact that, besides these two gases, oxygen also accumulates flammable impurities. These impurities create a risk of explosion that further complicates the separation process. In view of these difficulties, the authors of the study reported herein examined the process of separating krypton and xenon from the blowdown gases of the ammonia synthesis process (krypton and xenon enter the synthesis gas with air). The authors propose a process and equipment for obtaining a standard krypton-xenon mixture (99.5% Kr + Xe) from the methane fraction of the separation of ammonia synthesis blowdown gases based on low-temperature rectification in packed columns. This technology may be used to obtain an additional 960 m³ krypton and xenon (the cost of the pure products amounts to more than 1.2 million rubles) per each million tons of ammonia. The power expended per unit product during implementation of the new process was one-seventh of that expended during the conventional process of separating krypton and xenon from blowdown gases in large air separation units. The authors tested two types of packed columns under pressures ranging from 0.8 to 1.0 MPa in a two-stage separation process. A concentrate containing 0.3% krypton is formed during the first stage; in the second stage, this concentrate is used to obtain a krypton-xenon mixture containing no more that 0.5% methane. The column in the first stage includes exhausting and concentrating sections, which affords a high degree of krypton and xenon. The proposed unit (its design specifications are included) can process a methane fraction containing 2.8×10^{-3}% (Kr + Xe) at a rate of 2,200 m³/h. The new method does not require any new big equipment or extra service personnel and does not require the use of any other methods besides rectification. Figure 1; references 5 (Russian).

Optimizing the Continuous Commercial Process of Solution Crystallization of Matter

917M0109C Moscow KHIMICHESKAYA PROMYSHLENNOST in Russian No 1, Jan 91 pp 45-47

[Article by Yu.S. Ivchenko]

UDC 66.065.5.001.57

[Abstract] Each year the Soviet chemical industry produces hundreds of millions of tons of different crystalline substances by the method of crystallization from solutions. At present, most of the solution crystallization processes implemented involved the use of batch-type crystallizers. This equipment must be replaced by continuous equipment. Three types of continuous crystallization equipment exist: 1) devices entailing mixing of the suspension and extraction of nonclassified product; 2) devices entailing mixing of the suspension and extraction of classified product; and 3) devices that classify the suspensions by the size of the crystals growing in them and that permit extraction of classified product. The authors of the study reported herein have conducted a mathematical analysis of the dynamics of the process of continuous crystallization in the second and third of the three types of devices mentioned. In type 2 devices the suspension, which consists of crystals of different fractions, is repeatedly circulated through zones in which supersaturation of the solution carrying the growing crystals is created. Virtually all the growing crystals are formed under identical growth conditions. It is thus simplest to balance this process by equalizing the linear growth rate of the crystals of different fractions. In type 3 devices a supersaturated mother liquor is passed through the growing crystals. By filtering through the crystal layer from bottom to top, this mother liquor subjects the crystals to a pseudo-rarefaction and classifies them. This crystal growth process is best stabilized by equalizing both the volumetric and linear growth rates of the crystals of the different fractions. The best results are achieved by equalizing the linear growth rate of the crystals of the fine fractions and by equalizing the volumetric growth rate of the larger crystals. References 7: 5 Russian, 2 Western.

Standard Algorithms for an Automated Process Control System for Ion-Exchange Brine Cleaning

917M0109D Moscow KHIMICHESKAYA PROMYSHLENNOST in Russian No 1, Jan 91 pp 50-53

[Article by V.V. Yaroshevskiy and M.S. Rozenblyum]

UDC 621.3.035.82.012-52:681.306

[Abstract] This report is a continuation of the authors' study of the problems entailed in developing automated process control systems for the production of chlorine and caustic soda by the membrane method. Ion-exchange brine cleaning (deep cleaning in columns with ion-exchange resin) is used in membrane processes to ensure that the brine fed for electrolysis is of the highest quality with respect to its content of Ca^{+2} ions. In a previous study the authors of the work reported herein discussed the main stages and functions of an automated process control system developed to oversee the brine-cleaning process. In the present article they present control algorithms that make it possible to develop special software to execute the process control system's functions. Four algorithms are presented: an algorithm directing the operation of the automated process control system throughout all of the stages entailed in the deep-cleaning process, an algorithm to switch columns during the operating mode, an algorithm for logic program control of the regeneration of the resin and neutralization of the runoff, and an algorithm for logic program control of the preparation of diluted acid and alkaline solutions. Each of the algorithms presented calls for verification of the execution of the instructions issued by the control computer system. This is accomplished either on the basis of readings from the respective sensors or else on the basis of signals received from limit switches. The algorithms also provide for documentation of the control process, including output of messages to a printer or video display terminal. The algorithms also include provisions for the issuing of light and audio warning signals in the event of trouble in the process flow and for the disabling of the system's pumps. The authors conclude that introduction of their proposed algorithms will greatly reduce the manual labor entailed in the brine-cleaning process and greatly improve the quality of brine used for subsequent membrane electrolysis. Figures 5, table 1; references 2 (Russian).

Thermodynamic Optimization of Chemical Processes

917M0109E Moscow KHIMICHESKAYA PROMYSHLENNOST in Russian No 1, Jan 91 pp 54-56

[Article by V.A. Mironova]

UDC 66:536.7.001.57

[Abstract] The efficiency of chemical processes increases when the energy expenditures due to energy dissipation are reduced. The authors of this article attempt to show the results that may be achieved in the general case by reducing energy dissipation when several processes (specifically, chemical processes) are occurring simultaneously. They assume that the process under examination strays far enough from equilibrium for dissipative processes to develop while the medium remains homogeneous. Proceeding from the known fact that the amount of dissipated energy in such processes is proportional to the amount of entropy produced as a result of the processes' irreversibility, the authors proceed to

show that this quantity helps improve processes' efficiency indicators. They analyze the conditions of optimal organization of a chemical process for two scenarios: where the process proceeds near and far from equilibrium. They present optimization calculations for the process of producing AV-17-8 anion exchanger from a copolymer of styrene with divinylbenzene and trimethylamine in an amination department. According to their model, optimizing the process can reduce its duration by 16.6% (from 6 to 5 hours) and reduce raw material losses (the excess feeding of trimethylamine) by 26.6%. The authors state that analogous problems and solutions will also be valid for steady-state chemical processes occurring in an ideal displacement mode in a tube reactor. Figure 1; references 6 (Russian).

A Microprocessor System for Automatic Control With Protection Against Saturation

[Article by V.K. Naumkin, V.V. Podsevalov, and A.A. Frolov]

UDC 66.012.1

[Abstract] Because existing Soviet microprocessor controllers are either too narrowly geared toward a specific sector of industry or else too general in their orientation, the authors have developed an original automatic microprocessor chemical with protection against saturation. The new microprocessor controller is a digital controller the executes a proportional integral control law with protection against saturation (i.e., protection against a situation wherein the output imbalance signal exceeds the upper level of the standard signal range and either reaches the feed voltage value or drops to a value less than the lower level). The new regular executes an algorithm for saturation protection based on the output signal. This means that the controller's output signal can only vary within specified limits regardless of the amount of input imbalance. The microprocessor controller includes digital-to-analog and analog-to-digital converters, an Elektronika MK-64 computer, and a power supply unit. A series K145 LSI circuit system serves as the component base. The controller has a RAM to write the setup parameters and a ROM to store the algorithm of the proportional integral control law. A prototype of the new microprocessor controller was tested in the oxidation shop of the Azot Production Association in Shchekino. The controller was installed in the catalytic unit of the loop controlling the computation of the off (reaction) gases. The tests revealed that the new microprocessor controller is simple and convenient to service. It also improved the quality indicators of the process control system responsible for controlling the reaction gas-cleaning process. Eliminating the phenomenon of saturation made it possible to improve the quality of process control and also solved the problem of limiting the output signal within specified bounds. The new microprocessor controller has been recommended for use in different control loops at chemical enterprises requiring high-quality control, operating reliability, and easy servicing. Figures 3; references 5 (Russian).

Laws and Mechanism of Ignition of Hydrazine With Oxygen

[Article by V.V. Azatyan, T.G. Mkryan, E.N. Sarkisyan, and S.A. Chobanyan, Institute of Structural Macrokinetics, USSR Academy of Sciences, Moscow, and Institute of Chemical Physics, ArSSR Academy of Sciences, Yerevan]

UDC 541.11+541.126+546.171+546.21

[Abstract] The use of hydrazine in different areas of technology is complicated by the fire and explosion risk posed by hydrazine and air mixtures. In view of the importance of finding ways of reducing this risk, the authors of this article examine the existing information on the governing laws and mechanism of the ignition of hydrazine-oxygen mixtures. Specifically, they examine the following topics: features of the primary threshold of spontaneous combustion of hydrazine plus oxygen, chain branching reactions when hydrazine burns in oxygen, the participation of HO_2 radicals in linear chain-continuation reactions, kinetics of the reaction of hydrogen atoms with ignition and the breakdown of N_2H_3 radicals, self-inhibition of the combustion of hydrazine with oxygen; and an equation for the ignition threshold. They establish that the combustion and ignition of hydrazine with oxygen occurs in accordance with a branched chain mechanism. The main elementary reactions entailed in the process are identified. The phenomenon of self-inhibition in ignition processes is discovered, and self-inhibition is shown to be responsible for the very high primary thresholds of a large number of compounds. The authors further demonstrate that in a number of reaction systems in a wide pressure range, it is the competition of the branching of chains with their heterogeneous termination that is the decisive factor in ignition. This is the case despite the faster rates of some trimolecular reactions as compared with the rate of bimolecular branching. The authors conclude by presenting a set of reactions explaining the laws governing the ignition and burning of hydrazine with oxygen. They make particular note of the ninth and tenth stages of the reaction where a nonbranching chain of the decomposition of N_2H_4 without O_2 is formed. Figures 3; references 22: 18 Russian, 4 Western.

The Nature of Surface Modification by Potential Energy in Reactions of the Formation and Breakdown of HCOO⁻-Me⁺ Ion Pairs

[Article by A.M. Kariyev and A.A. Ovchinnikov, Institute of Chemical Physics imeni N.N. Semenov, USSR Academy of Sciences, Moscow]

UDC 539.194:541.6

[Abstract] Ion channels that are capable of transporting alkali metal cations are observed both in biological objects (excited biomembranes) and in the world of inorganic chemistry (in superionic conductors). In view of the importance of such channel structures in molecular biology and physical chemistry, the authors of the study reported herein examined the nature of surface modification by potential energy in reactions of the formation and breakdown of HCOO⁻-Me⁺ ion pairs. They used the nonempirical quantum chemistry method of the self-consistent theory of molecular orbitals in a linear combination of atomic orbitals of Hartree, Fock, and Rutan in a two-exponent Dunning basis plus an expanded set of Huzinaqa-Dunning gaussian functions to perform a series of calculations related to the following complexes: HCOO⁻-Na⁺-H, HCOO⁻-K⁺Na⁺, and HCOO⁻-H_2O-Na⁺. They also made a series of calculations for HCOO⁻-Na⁻, HCOO⁻-Li⁺, and HCOO⁻-Li⁺-H⁺. In these latter calculations, consideration is given to the electron correlation based on the Moller-Plesset theory of second-order excitations. The specified basis is supplemented with polarization functions of the d-type at the oxygen atom and with functions of the p-type at the hydrogen atom, as well as with diffusion functions of the p-type at the oxygen atom. It is shown that introducing water molecules between oppositely charged ions destabilizes the HCOO⁻-Na⁺ pair much more strongly than does the ion-ion interaction that occurs in HCOO⁻-2Na⁺. It is hypothesized that in the case where two metal cations are simultaneously located in an aqueous ionic channel, the modification of the potential ion transfer barriers does not entail any electrostatic interaction between ions. Rather, it entails the exchange of water molecules from the coordination sphere of oppositely charged ions. Figures 6, table 1; references 45: 17 Russian, 28 Western.

The Effect of Heat Losses on Combustion in a One-Dimensional Flow

[Article by A.I. Mamedov, G.B. Manelis, S.I. Khudyayev, and G.V. Shkadinskaya, Chemical Physics Institute imeni N.N. Semenov, USSR Academy of Sciences, Chernogolovka]

UDC 536.46

[Abstract] Interest in frontal modes of chemical transformation in a reagent flow is dictated above all by the design and technology of frontal-action flowthrough chemical reactors. When designing a reaction that is to occur in a stationary mode it is crucial to know the location of the reaction zone and the effect that such key external parameters as reagent feed rate and heat loss intensity will have on it. Although the literature on this topic is extensive, it largely ignores side heat losses. For

this reason, the authors of the study reported herein examined the effect of heat losses on combustion in a one-dimensional flow. They have used the asymptotic approach, which although extensively developed abroad, is still rarely encountered in the domestic literature. They develop a series of 50 equations, and manage to determine the conductive combustion thresholds, the effect of side heat losses on the heat flow through the plane z = 0, and the position of the reaction zone. The also identify four characteristic regions of temperature change. Figures 3; references 12: 6 Russian, 6 Western.

An Investigation of the Reactivity and Ignition Mechanism of Spiro Compounds

[Article by G.V. Bakulina, Ye.V. Bespalov, O.D. Kazakov, Ye.S. Severin, V.G. Slutskiy, A.M. Tereza, and S.A. Tsyganov, Institute of Chemical Physics imeni N.N. Semenov, USSR Academy of Sciences, Moscow]

UDC 541.124.13

[Abstract] Because of their extended stability, spiro compounds (spirans), i.e., saturated hydrocarbons with intense C-C bonds, are promising for use in power plants. For this reason, the authors of the study reported herein conducted an experimental study of the reactivity of very simple mono- and bicyclic spiro compounds and analyzed their ignition mechanism. They studied the reactivity of stoichiometric air mixtures of mono- and bicyclic spiro compounds at temperatures ranging from 1,100 to 1,160 K. The structure of the spiro compounds was found to have a significant effect on their reactivity. A correlation between spiro compounds' structure and chemical activity, as well as with the activity of the products of spiro compound's thermal breakdown, was also determined. It is shown that those spiro compounds that have ethylene and butadiene as their destruction products are the ones with maximal activity. The authors go on to propose a kinetic mechanism explaining this phenomenon. Figures 6, tables 2; references 18: 5 Russian, 13 Western.

The Ignition of Surface-Heated Condensed Matter During the Occurrence of Two Competing Exothermal Reactions

[Article by K.Yu. Voronin and B.S. Seplyarskiy, Kuybyshev Polytechnic Institute imeni V.V. Kuybyshev]

UDC 536.46:517.94

[Abstract] Using the methods of the classical theory of combustion to calculate ignition characteristics when several reactions are occurring in a substance results in serious problems. In an effort to solve this problem, the authors of the study reported herein examined the process of the ignition of surface-heated condensed matter during the occurrence of two competing exothermal reactions. They base their work on the following model. On the boundary of a semi-infinite condensed substance at some initial moment in time, the temperature instantaneously reaches the substance's ignition temperature and remains unchanged during the course of the entire process. The heating of the substance triggers an intensive chemical reaction that results in combustion. It is assumed that the reactions result solely in the formation of condensed products and that there are no phase transitions. The chemical transformation proceeds in accordance with zero-order reactions, and the rate of the reactions at the initial temperature is infinitesimally small. In a previous communications, one of the two authors (B.S. Seplyarskiy) of the present study proposed a method for calculating ignition characteristics based on the wave mechanism of the formation of a chemical reaction zone. This method is used to calculate the main characteristics of the ignition process (time of inert heating, time required to establish thermal equilibrium, time to ignition, and coordinate of the break from thermal equilibrium). The authors proceed to analyze the dependence of the ignition process' time characteristics on heating temperature, and they create a system for classifying ignition modes. The proposed wave mechanism of the formation of a chemical reaction zone enables the authors to determine the minimal time of a heater effect in the case of pulsed energy feed. The authors also manage to the confirm B.S. Seplyarskiy's previously published physical pattern of the ignition process and recommend it for use in calculating ignition characteristics when the transformation of the starting substance is described in terms of complex chemical transformations. Figures 3; references 10 (Russian).

The Reaction of Sulfur With Metals During Shock Loading

[Article by M.F. Gogulya, I.M. Voskoboynikov, A.Yu. Dolgoborodov, N.S. Dorokhov, and M.A. Brazhnikov, Institute of Chemical Physics imeni N.N. Semenov, USSR Academy of Sciences, Moscow]

UDC 539.63

[Abstract] The problems associated with the occurrence of solid-phase reactions during shock loading have long attracted researchers' attention. The authors of the study reported herein examined the possibility of the occurrence of an exothermal reaction behind a shock wave front in pressed specimens of mechanically mixed sulfur and metal measuring 50 mm in diameter and 3 mm in height. They created shock waves in the specimens by

detonating TG 50/50 shells on the specimens' faces at a density of 1.67 g/cm^3. The following composites were studied (figures in parentheses indicate their weight ratios): Mg/S (43/57), Mg/S (63/37), Al/S (55/45), Ti/S (60/40), Fe/S (54/46), Cu/S (66/34), and LiF/S (35/65). The resultant dependences of the changes in effective brightness temperatures on the contact boundaries with the window materials indicate the presence of a reaction directly behind the shock wave front after a time on the order of 50 ns for the mixtures of sulfur with Mg, Al, and Ti. A conservative estimate of the degree of transformation for the system Mg/S amounts to about 0.2, and for Al/S it amounts to about 0.5. A qualitative agreement between the calculated and experimental pressure profiles was observed. Figure 1, table 1; references 6: 4 Russian, 2 Western.

Cathodic Evolution of Hydrogen From Acid Solutions in Light and Heavy Water

[Article by L.B. Kriksunov, L.I. Krishmalik, and V.M. Tsionskiy, Electrochemistry Institute imeni A.I. Frumkin, USSR Academy of Sciences, Moscow]

UDC 541.138.3

[Abstract] Previous research on the cathodic evolution of hydrogen from acid solutions in light and heavy water has revealed that the overvoltages occurring in heavy water are substantially higher (130 mV higher in one study and 70-90 mV higher in another) than those occurring in light water. Previous studies have also revealed that this difference decreases as the reaction temperature is increased and that the difference in the rates of the two reactions increases as the overvoltage increases. In Tafel coordinates this effect is manifested in a slight difference in the slopes of the reactions' polarization curves. Because this fact is difficult to reconcile with the reduced isotope effect measured in a protium-tritium mixture in acid solutions, the authors of the study reported herein examined the cathodic evolution of hydrogen from acid solutions in light and heavy water. They measured the polarization curves of the cathodic evolution of light and heavy hydrogen from acid aqueous (H_2O and D_2O) solutions on mercury at temperatures from 110 to 240°C. They compared the reaction kinetics in H_2O and D_2O not only in the range of the conventional discharge (as was done in previous studies) but also in the range of the barrierless discharge of hydrogen ions. These phenomena were then compared with the isotope effect observed during the electrolysis of an isotope (protium and tritium) mixture. Analysis of the resultant data revealed that the convergence of the reagents plays an important role in the slow discharge of hydroxonium ions. This convergence is determined to be dictated at least partially by the forces restraining the donor protons in the solution. The electrode field is also found to act upon these forces in a manner depending on the properties of the medium. The authors further discovered that the isotope effect virtually disappears in the region of the transition from a conventional to a barrierless process. Figures 3, table 1; references 20: 9 Russian, 11 Western.

The Electron-Donor Approach to the Interaction Occurring Between Cations and Biologically Active Substances and Membranes

[Article by R. Notoya and A. Matsuda (deceased), Hokkaido University and Catalysis Institute, Cannopo, Japan]

UDC 541.13

[Abstract] In view of the importance of metal cations in biological processes the authors of the study reported herein used the electron donor-acceptor approach to examine the interaction between cations and biologically active substances. Specifically, they set out to show that the bond in complexes of amino acids, adenosine triphosphate, imidazole, etc., including the membrane-cation bond, occurs as a result of an electron donor-acceptor interaction and is determined by the absolute basicity of these ligands. They derive two empirical rules governing this interaction and calculate the relative correlations for the energies of ion solvation and haloid dissociation of metals and organometallic compounds. These rules are used to describe the interaction occurring between amino acids, nucleic acids, and metal cations. The results obtained show that the interactions between biologically active substances and cations have a donor-acceptor nature. The interaction of nucleic acids with membranes in the presence of cations is also discovered to be dictated by the acidities of these cations. Nine basic equations related to complexing in the biologically active substances and membranes studied are also presented. Figures 11, tables 2; references 12 (Russian).

Additional Analysis of the Adsorption and Kinetic Effects in Cesium Salt Solutions at a Mercury-Water Interface

[Article by B.B. Damaskin and V.A. Safonov, Moscow State University imeni M.V. Lomonosov]

UDC 541.13-183

[Abstract] In previous publications the authors of the present study examined the electrochemical behavior of the system Hg/[H_2O + mc M CsA + (1 - m) cM LiA], where A⁻ represents Cl⁻ or F⁻. In that study they showed that for ε_1 = 33, regardless of whether anions do or do not enter the region $x_2'x_2''$, the totality of adsorption and kinetic effects in cesium salt solutions at the Hg-H_2O interface cannot be entirely reduced to a combination of geometric and purely electrostatic factors but that assumptions regarding some specific adsorption of Cs⁺ cations is also necessary. In the study reported herein, they continue their research at even lower values of ε_1. The study is conducted within the framework of the Fawcett model assuming two positions of the external Helmholtz plane (x_2' and x_2'') for different electrolyte ions. The experiments conducted reveal that the shift in the zero-charge potential of the Hg electrode that is observed in aqueous CsF solutions is much greater than the calculated values of ΔE_{q-0} at all values of the dielectric constant ε_1 in the region $x_2'x_2''$. It is further shown that the version of the Fawcett model with a reduced ε_1 value is internally contradictory owing to the

effect of representation forces. Figures 7, tables 3; references 14: 9 Russian, 5 Western.

The Electrochemical Behavior of Polycyclic Arenes—Activators of Peroxide-Oxalate Chemiluminescence. Oxidation of Substituted Naphthalenes and Anthracenes on a Platinum Disk Electrode

[Article by O.A. Antonkina, Ye.V. Kryukova, S.K. Smirnov, V.M. Shershukov, S.F. Kramarenko, I.B. Nemchenok, L.N. Veselova, and A.P. Tomilov, State Union Scientific Research Institute of Organic Chemistry and Technology, Moscow]

UDC 541.138.2:547.6:535.379

[Abstract] Peroxide-oxalate chemiluminescent composites are used extensively in creating safe light sources and in luminescence analysis. These composites generally consist of a reagent (oxalic acid ether), hydrogen peroxide, principal catalyst, activator (luminophor), and solvent. Polycyclic arenes, i.e., naphthalene, anthracene, and tetracene derivatives, are generally used as luminophors. The authors of the study reported herein conducted a comparative analysis of the electrochemical oxidation of substituted naphthalenes and anthracenes on a platinum disk electrode in an anhydrous medium. They examined the connection between the structure of the aforesaid compounds and their oxidation potentials and spectral-luminescence properties. The data obtained by the authors regarding the electrochemical oxidation of naphthalene and anthracene were found to be in good agreement with other published data on these compounds. Because the authors of the present article were the first to systematically study the electrochemical behavior of the other 12 compounds studied, their results regarding those compounds could not be compared with others' work. The authors discovered that during the first stage of the electrochemical oxidation of naphthalene and anthracene and their derivatives, the electron at the carbon atom in the respective positions 1(4) or 9(10) characterizing the greatest electron density breaks away. The stability of the resultant cation-radicals is higher in the case of anthracene than in the case of naphtalene and depends on the nature of the substituents surrounding the reaction center. the cation-radical 9,10-diphenylanthracene is one of the most stable. For 9,10-bis-(phenylethynyl)-anthracene and its derivatives, the authors discovered a correlation between $E_{1/2}(Ox)$ and

the σ-constants of the substituents based on the Hammett-Zuman equation. Figures 5, tables 3; references 29: 8 Russian, 21 Western.

Thermodynamics of the Formation of Highly Conductive Phases of Alkali Earth Metal Fluorides

[Article by R.M. Guseynov and V.D. Prisyazhnyy, Dagestan State Pedagogical Institute, Makhachkala, and Institute of General and Inorganic Chemistry, UkSSR Academy of Sciences, Kiev]

UDC 541.135.4

[Abstract] At high temperatures, crystalline fluorides of rare earth metals with a fluorite structure (CaF_2, SrF_2, and BaF_2) are characterized by an anomalous alteration in their transport and thermodynamic characteristics. Elsewhere it has been proposed that this behavior is due to the intensive disordering of the anion sublattice (quasi-fusion) that occurs in some temperature interval all the way to the melting point of the crystalline phases. The authors of the study reported herein have attempted a theoretical calculation of the thermodynamic parameters of the phase transitions of rare earth metal fluorides into a high-conductivity state. They have done so by proceeding from a model of these fluorides' gradual anionic disordering. The following parameters are considered: configurational entropy, free energy of defect formation, and percentage of free energy associated with anionic defects in accordance with Frenkel. Among other things, the calculations performed indicate the following: 1) fluorine anions are the main current carriers in both the solid and liquid phases, and 2) the degree of disordering of the anionic sublattice m increases in proportion to the lattice parameter a (adjusted for room temperature) and the size of the cation or else to the ratio of the radii of the cation and anion. These and other results obtained by the authors have led them to conclude that the model of the gradual temperature disordering of the anionic sublattice provides a satisfactory explanation of the anomaly of the transport and thermodynamic properties of alkali earth metal fluorides with a fluorite structure. The authors further state that their results may also be extended to other compounds with a fluorite and antifluorite structure (including alkali earth metal chlorides and oxides of the type ZrO_2 and ThO_2). Tables 2; references 6 (Russian).

Reflection of Light From Small Regular Irregularities

[Article by R.Z. Vitlina, Institute of Semiconductor Physics, Siberian Department, USSR Academy of Sciences]

UDC 535.016

[Abstract] The reflection of waves from a rough surface has been the subject of many works. Included among these are a line of works focused on a regular type of irregularity. The author of the study reported herein has continued research in this direction, focusing on the reflection of light by a periodically corrugated surface that is the interface between two dielectric media. The irregularity studied is assumed to be small in comparison with the wavelength of the incident radiation in these media. The form of the irregularities and ratio of the dielectric constants of the media are arbitrary. The reflected field is proportional to the area-averaged field under one irregularity. It is found by using a system of integral equations. In the case where the ratio of dielectric constants of the two media is large, the determination of the reflection factors may, depending on the slope of the contour, include one unknown that depends solely on the geometry of the irregularity. The problem examined is said to be reminiscent of the problem of the problem of the potential of a zero radius in quantum mechanics inasmuch as the wave function is, in a small region, characterized by some quantity that is the problem variable (in this case the average field under the irregularity). References 7: 5 Russian, 2 Western.

The Effect of Thin Dielectric Films on the Spectra of Light Scattering by Surface Acoustic Waves

[Article by V.N. Yegorov, V.V. Lavrik, I.L. Chistiy, and V.T. Shunyakov, Donetsk Physical Technical Institute, UkSSR Academy of Sciences]

UDC 535.361

[Abstract] The scattering of light on warm surface acoustic waves makes it possible to study the distinctive features of the propagation of surface elastic waves in a solid at hypersonic frequencies and is a powerful method of studying the physical, mechanical, and thermal properties of a solid's surface. Other researchers (including Sandercock) have conducted experimental studies of the scattering of light on warm surface acoustic waves in a number of materials and have obtained scattering spectra by using the technology of a Fabry-Perot ultra-contrast multipass interferometer. These results mainly illustrated the feasibility of a Fabry-Perot interferometer, and their interpretation was left as a subject for further analysis. One particular aspect of these studies that (according to the authors of the study reported herein) warrants further examination is the fact that the experimental values of the speed of sound obtained when using Sandercock's dependence of the propagation velocity of a surface acoustic wave in an Si crystal from the direction of the sound to the surface (001) are very different from those calculated theoretically under the assumption of a free silicon surface. In view of this discrepancy, the authors of the study reported herein conducted a theoretical examination of the effect of a thin dielectric film on the acoustic properties of a solid's surface and used the results of their theoretical examination to interpret Sandercock's results. The author's obtain a theoretical value for the speed of a Rayleigh wave on a surface without a film in the direction (100) of 49.2×10^5 cm/s as opposed to the figure 47.9×10^5 cm/s reported by Sandercock. In other words, they determined that the film thickness in Sandercock's work amounted to about 32 angstroms. This result is in good agreement with the results of ellipsometric measurements of the thickness of natural SiO_2 oxide on the surface of crystalline Si specimens. The proposed method is recommended for use in determining the decrease (increase) in the velocity of surface acoustic waves in cubic crystals caused by the presence of thin dielectric films on the crystal's surface. Figure 1; references 8: 4 Russian, 4 Western.

Effective Product Temperature During Laser Vaporization and Desorption

[Article by A.N. Mezhuyev, B.S. Podolskiy, V.A. Kuraintsev, and A.A. Chernov, Crystallography Institute, USSR Academy of Sciences, Moscow]

UDC 541.183+541.145

[Abstract] Time-of-flight spectroscopy is one of the few methods that can be used to study the elementary processes occurring during pulsed laser vaporization and desorption. More than once has the method provided extremely interesting information regarding the physicochemical processes occurring on a surface subjected to pulsed laser radiation. The results obtained by time-of-flight spectroscopy do not, however, always lend themselves to clear and unequivocal explanation. This is particularly true in the case of the link between the effective temperature of products determined from a time-of-flight spectrum and the parameters of the actual process. The authors of the study reported herein conducted an experimental study of the laser vaporization of silicon film oxidized in water vapors. The experiments

were conducted in an ultrahigh vacuum chamber with a residual gas pressure of about 10^{-8} Pa. The pressure was measured by a VI-14 ionization vacuum gauge, and a QMG-511 quadruple mass spectrometer (Balzers) was used to determine the makeup of the gases. A 128-channel pulse analyzer with a counting speed of about 1.4×10^6 pulses per second and a maximal channel-switching frequency of about 100 kHz were used as the mass spectrometer operating in an ion-counting mode. The radiation of a YAG:Nd^{3+} laser operating in a single mode (TEM$_{00}$) was fed into the vacuum chamber through a sapphire window and focused on the specimen in a spot with a diameter of about 1.5 mm. The radiation had a wavelength of about 1.06 μm and a half-height pulse duration of about 5 +/- 1 ns. The pulse energy was varied by using neutral light filters and measured by an IMO-2N calorimeter directly in front of where the beam entered the vacuum system. A significant difference between the effective desorption temperature of SiO (about 6,000 K) and H$_2$ (about 500 K) was discovered. The researchers then developed a numerical model of the processes of laser vaporization and desorption and analyzed the gas dynamic dispersion of the products formed. It was established that even in the case of thermal laser vaporization and desorption, the effective product temperature may differ significantly from the maximal surface temperature. Figures 6; references 17: 8 Russian, 9 Western.

The Change in the Structure of Niobium When It Is Irradiated With Oxygen Ions

[Article by R.N. Kekanosidze, E.M. Diasamidze, B.G. Eristavi, N.I. Mausuradze, E.R. Kuteliya, A.V. Sichinava, and N.Ye. Menabde, Georgian Polytechnic Institute, Tbilisi]

UDC 539.213:621.382

[Abstract] Elsewhere it has been shown that polycrystalline Nb implanted with O$^-$ ions in a dose of 1×10^{18} cm^{-2} at an energy of 100 keV and annealed in a vacuum at 1,200°C yields an emission current density that is 2.5-fold that of pure niobium. Out of an interest in the reason behind this phenomenon, the authors of the study reported herein examined the change in the crystalline structure of O$^-$ ion-doped monocrystalline Nb(110) and its dependence on annealing temperature. The specimens were prepared in accordance with the standard method for ion implantation doping. They were alloyed at room temperature in a system with a cryogenic sheath under liquid nitrogen in doses from 1×10^{16} to 1×10^{18} cm^{-2} at an energy of 100 keV. They were then subjected to heat treatment in a vacuum of 3×10^{-5} Pa for 30 minutes at each temperature value. The ion-doped layers were analyzed by the methods of secondary ion mass

spectrometry and electronography in the temperature range from 200 to 1,400°C. The profiles of oxygen distribution throughout the depth of the implanted layer were determined on an LAS-2000 at an argon ion energy of 5 keV and a current density of 2×10^{-5} A-cm^{-2} based on the yield of negative oxygen ions. Bombardment was found to result in amorphization and a volumetric increase in the ion-doped layer. Niobium dioxide with an ordered tetragonal structure was found to form during the annealing process between 200 and 800°C. At 1,000°C the NbO$_2$ breaks down, and the body-centered lattice of the niobium is restored. Figures 3; references 9 (Russian).

The Effect of Surface Roughness on the Optical Constants of Materials Produced From Reflection Spectra

[Article by B.V. Andriyevskiy, V.Yu. Kurlyak, N.A. Romanyuk, and I.V. Stus, Lvov State University]

UDC 538.958;538.971

[Abstract] Determining the optical constants of crystals from mirror-reflection spectra requires the manufacture of smooth surfaces. It is a well-known fact that the presence of surface roughness of a surface-contaminating film can change experimental reflection spectra and the optical constants calculated on their basis. The authors of the study reported herein proceed from the scalar theory of the interaction of light with a rough surface to develop a model calculation of the effect of the magnitude of roughness on the change in the mirror reflection factor and (based on Kramers-Kronig transforms) on the change in the optical constants of K$_2$SO$_4$ monocrystals in a broad region of the VUV spectrum of their natural absorption, 7 to 22 eV. They base their model calculations on the following formula for the interaction of light with a reflective surface: $R/R_0 = \exp(-16\pi^2\sigma^2/\lambda^2) + [1 - \exp(-16\pi^2\sigma^2/\lambda^2)] \times [1 - \exp(-16\pi^2\sigma^2\gamma^2/\lambda^2)]$, where R$_0$ is the reflection factor of an ideally smooth surface; R is the reflection factor of a rough surface; σ is the mean square height of the irregularity of the rough surface; λ is the wavelength of the light; $\gamma = \beta l$ times (2 times the square root of 2σ)$^{-1}$; β is the aperture angle; and 1 is the correlation length of the surface roughness. According to this formula, the effect of roughness σ on the mirror-reflection factor is greater as the wavelength of the measurement is smaller. This dependence is monotonic. The results of experimental measurements taken by the authors led them to conclude that the aforesaid formula cannot be generally used to calculate the reflection factor of an ideally smooth surface and the respective differential optical constants in that region of the spectrum where a marked structure is observed. The formula may,

however, be used to calculate the effect of surface roughness on integral constants. It must, however, be borne in mind that the parameter σ in this formula must be increased somewhat in comparison with the actual geometric surface roughness parameter so as to include the mechanism of the dissipation of the electron excitation in the light-scattering process. Figure 1, table 1; references 5: 3 Russian, 2 Western.

The Wear Resistance of Bronze Operating in a Jet Fuel Medium After Argon Implantation

[Article by N.Ye. Galat, V.A. Zuyev, B.N. Romanov, and L.P. Khlistun, Kiev Tank Institute of Higher Learning]

UDC 621.785.5.048.7

[Abstract] The problem of surface implantation microordering of metals has recently attracted a great deal of attention. Most such works deal with the implantation of ions resulting in a radiation effect and/or in the formation of new phases and chemical compounds. In a continuation of this line of research, the authors of the study reported herein examined construction materials operating in a medium of low-molecular-weight carbon jet fuel. They use specimens made of Br05Ts5S5 bronze as their test samples and specimens of ShKh15 steel as controls. The specimens were subjected to bombardment with Ar^+ in a dose of 10^{16} cm^{-2} at an energy of 75 to 125 keV. Their wear resistance in jet fuel was determined in a laboratory linear contact friction instrument. The test conditions were as follows: fuel temperature, 293 K; glide speed, 0.03 m/s; friction path, 1,000 m; and initial maximal specific load, 100 kgf/mm^2 for the bronze specimens and 200 kgf/mm^2 for the steel specimens. The distribution of the different chemical elements on the friction paths was determined by an MZ-46 x-ray microprobe and analyzed by computer. Before argon implantation the bronze had a wear of 0.052 mm; this figure decreased by 12% after implantation at an energy of 75 keV and by 40% after ion bombardment with an energy of 125 keV. The steel had pre- and postimplantation wear values of 0.005 mm and 0.0025 nm, respectively. Analysis revealed that the implanted bronze specimens' oxygen content in the zones of the friction paths was less than that of the nonimplanted specimens by a factor of 3.5. The sulfur content in these same ion-implanted specimens was a factor of 2.5 less than that in the nonimplanted specimens. These preliminary tests thus confirmed that implanting argon ions in bronze to be used in a jet fuel medium exerts a significant effect on the bronze's wear resistance. References 7: 6 Russian, 1 Western.

Investigation of the Kinetics of the Dehydrogenation of Propane on Aluminoplatinum Catalysts

[Article by Lyu Kam Lok, N.A. Kayday, S.L. Kuperman, Kho Shi Tkhoang, N.M. Podkletnova, and S.B. Kogan, Institute of Organic Chemistry imeni N.D. Zelinskiy, USSR Academy of Sciences, Moscow, and Lenneftekhim (VNIINeftekhim Scientific Production Association, Leningrad]

UDC
541.128.13:541.127:542.941.7:547.213:546.92'623

[Abstract] Platinum systems are highly effective paraffin dehydrogenation catalysts. In previous communications, the authors of the study reported herein examined the kinetics and mechanism of the dehydrogenation of isobutane and n-butane on aluminoplatinum catalysts containing 0.35% Pt without a promoter and with selenium, lead, copper, germanium, indium, and tin additives. In the present article they examine the kinetics and mechanism of the dehydrogenation of propane (i.e., $C_3H_8 = C_3H_6 + H_2$) on various aluminoplatinum catalysts. The experiments were conducted at atmospheric pressure in the presence of hydrogen in a flowthrough circulation unit that has been described elsewhere. Three catalysts were used: Catalyst 1 contained 0.6% Pt and 1% K on type A-64 γ-Al_2O_3. In addition to the elements present in catalyst 1, catalysts 2 and 3 each contained either 2% Sn or In, respectively. Between 2.0 and 3.5 g catalyst was loaded into the reactor. The reaction mixture was analyzed on an LKhM-8MD chromatograph with a katharometer and a silica gel-filled column 0.7 m long. The kinetic isotope effects were measured by comparing the rates of reactions in the presence of hydrogen and deuterium under identical conditions as the conversion and temperature were kept unchanged. The reaction kinetics were studied in the temperature range from 570 to 620° at initial partial propane pressures of 167 to 760 gPa, initial partial hydrogen pressures of 0 to 670 gPa, and initial partial pressures of the added propylene ranging from 0 to 333 gPa. The total degree of propane transformation ranged from 0.08 to 0.50. The selectively of transformation of propane into propylene ranged from 0.61 to 0.99. The degree to which equilibrium was approached under the test conditions ranged from 0.21 to 0.90. A corrective factor γ, which was calculated from equilibrium constant values published elsewhere, was used to give consideration to the reverse reaction. Under the conditions studied, the equilibrium output of propylene ranged from 0.34 to 0.65. It was assumed that the stoichiometric number of the limiting stage equaled 1. The reaction occurred in the kinetic region on catalyst granules less than 2 mm in size. The researchers measured the kinetic isotope effects when hydrogen was replaced by deuterium in forward and reverse reactions. The presence of Sn and In in aluminoplatinum catalysts

was found to increase the propylene formation rate by factors of 3.2 and 4.6, respectively. Catalyst 1 was found to have a selectivity of 0.79, whereas catalysts 2 and 3 had selectivities of 0.96-0.97. The authors then proposed a kinetic equation describing the experimental data in a broad range of process parameter variation. The four-stage scheme of the reaction was substantiated. This substantiation resulted in a kinetic equation that is in good agreement with the experimentally determined data. Figures 3, table 1; references 11: 10 Russian, 1 Western.

Analysis of the Process of Hydrogenation of Benzene on a Pt/Al$_2$O$_3$ Block Honeycomb Catalyst

[Article by N.M. Ostrovskiy, A. Parmaliana, F. Frusteri, L.P. Maslova, and N. Dzhordano, Omsk Department; Catalysis Institute, Siberian Department, USSR Academy of Sciences; Industrial Chemistry Institute, Messina University, Italy; and TAE-Chinese People's Republic Institute, Messina, Italy]

[Abstract] Other researchers have proposed that honeycomb blocks be used as a carrier for a platinum benzene hydrogenation catalyst in hydrogen accumulation processes. These same researchers made thermodynamic estimates of the effectiveness of this accumulation method and examined the kinetic laws governing the transformation of benzene on applied block catalysts. In a continuation of this line of research, the authors of the study reported herein examined the kinetics of the hydrogenation of benzene on a Pt/Al$_2$O$_3$ honeycomb block catalyst. A portion of the tests were conducted in a gradientless flowthrough circulation reactor using a 0.5% Pt/γ-Al$_2$O$_3$ catalyst at temperatures between 150 and 230°C with an H$_2$:B molar ratio of 4.3 in accordance with a method described elsewhere. The other portion of the experiments were conducted on a 0.21% Pt/γ-Al$_2$O$_3$ block catalyst in an integrated reactor in accordance with a method described yet elsewhere. These latter experiments were conducted at temperatures between 150 and 250°C, with a benzene contact time of 2 to 100 (g x h)/mol and with an H$_2$:B ratio between 3 and 10. The results of both sets of experiments were used to construct two kinetic models of the kinetics of reaction kinetics. A comparison of the models developed and the experimental data indicated that the two models described the actual processes with errors of of 7.5 and 9%, respectively. The authors proceeded to assess the possibility of implementing the process in a multilayer adiabatic reactor. Figures 4, table 1; references 24: 8 Russian, 16 Western.

Investigation of Catalysts and Catalytic Combustion Reactions. VII. The Effect of Macrodefects on the Strength Characteristics of Al$_2$O$_3$—A Carrier of Catalyst for Catalytic Heat Generators

[Article by M.N. Shepeleva, Z.R. Ismagilov, I.A. Ovsyannikova, and G.I. Goldenberg, Catalysis Institute, Siberian Department, USSR Academy of Sciences]

[Abstract] The development of work related to catalytic heat generators has increased the requirements regarding the strength and wear resistance of catalyst granules. Because the structural and mechanical properties of catalysts are largely determined by the properties of their carriers, there is an obvious need to create a catalyst that, besides having a well-developed surface and porosity, is also capable of operating under the conditions of a fluidized bed. Other researchers have demonstrated the possibility of producing Al$_2$O$_3$ (a carrier of catalytic heat generator catalysts) with variable structural and mechanical characteristics by forming it into spherical granules by the fluidization method. The authors of the study reported herein have worked to establish the reasons for the production of Al$_2$O$_3$ granules with sharply differing strength indicators depending on their processing conditions. They studied three series of specimens prepared in different manners. In the series 1 specimens they used nitric (specimen 1) and acetic (specimen 2) acids, which differ with respect to their capability of peptizing the initial aluminum hydroxides. In the series 2 specimens they varied the formation conditions by using ammonia solutions that were either rather concentrated (specimen 3) or diluted (specimen 4). In producing the series 3 specimens they varied the drying conditions by using both soft drying conditions while holding the granules to dry for an extended period (specimen 5) and rigid conditions, i.e., removing a large amount of moisture within 30-40 minutes (specimen 6). By using scanning electron microscopy and x-ray microanalysis, the authors managed to demonstrate that even slight deviations form optimal synthesis conditions can lead to significant reductions in granule strength, primarily due to the formation of internal macrodefects. The changes occurring in such indicators as specific surface, pore size, and bulk density were not nearly as significant as were the changes in granule strength (the latter ranged from a factor of 1.5 to a factor of 3). Figures 3, table 1; references 13: 12 Russian, 1 Western.

Investigation of Catalysts and Catalytic Combustion Reactions. VII. A Study of the Change in the Nature of Contacts Between Primary Particles in Aluminum Hydroxides Subjected to Milling

[Article by M.N. Shepeleva, E.R. Ismagilov, R.A. Shkrabina, E.M. Moroz, V.B. Fenelonov, and V.I. Zaykovskiy, Catalysis Institute, Siberian Department, USSR Academy of Sciences]

UDC 541.128.35:546.623-36:539.21'89

[Abstract] In a continuation of the long line of research on the production of Al_2O_3 catalysts, the authors of the study reported herein examined the possibility of changing the nature of the contacts among primary aluminum hydroxide particles during milling and the possibility of using aluminum hydroxide produced from mechanically activated aluminum hydroxide to create ultrastrong granulated carriers for catalytic heat generator catalysts. Commercial coarsely dispersed aluminum hydroxide with a pseudo-boehmite structure and a moisture content of 73% by weight was selected as the starting material. The hydroxide was treated with acid to produce a plasticized mass possessing fluid properties. The fluidization method was then used to form the mass into spherical granules in an ammonia solution-filled column. γ-Al_2O_3 was obtained after drying and roasting. The specific surfaces of the aluminum hydroxide and Al_2 were determined (at 110° and 600°, respectively) by the method of thermal desorption of Ar, their pore volumes and pore radii were determined by mercury pyrometry, and their phase composition and dispersion of primary particles were determined by using a DRON-1.5. Electron microscopy and mechanical strength studies were also performed. The studies demonstrated that milling starting aluminum hydroxides does indeed change the nature of the contacts between primary particles. The transition of the phase contacts into weak coagulation contacts permits deep disaggregation of the aluminum hydroxides under the action of a peptizing acid. This in turn results in strong and dense Al_2O_3 granules to serve as catalyst carriers in fluidized bed processes. Figures 3, tables 2; references 8: 7 Russian, 1 Western.

The Complexing and Decomposition of N_2O on Bronsted and Louis Acid Centers of High-Silica Zeolites: A Spectral and Quantum Chemical Investigation

[Article by V.L. Zholobenko, I.N. Senchenya, L.M. Kustov, and V.B. Kazanskiy, Institute of Organic Chemistry imeni N.D. Zelinskiy, USSR Academy of Sciences, Moscow]

UDC 541.128.13:541.183:549.67:546.172.5:542.924:-543.422.4:539.196

[Abstract] N_2O is currently used in a variety of ways. It is used as an oxidizing agent to activate lower paraffins so as to partially oxidize or dehydrate them. The reaction of the decomposition of N_2O is also used as a model for studying the redox properties of zeolites and oxides, and the molecule N_2O can also be used as a spectral test. In view of the many uses of N_2O, the authors of the study reported herein use the IR spectroscopy method to study the interaction of N_2O with Louis and Bronsted acid centers of type HZSM-5 decationized zeolites. They produced HZSM-5 (SiO_2/Al_2O_3 = 40) zeolite by acid treatment of the Na form. The specimens were subjected to preliminary activation by thermal vacuum treatment at 450 to 850°C for 4 hours. Perkin-Elmer 580B and Acta M-VII Beckman spectrophotometers were used to measure the zeolites' IR spectra in diffusely scattered light in the range from 2,000 to 5,000 cm^{-1}. As a test to identify the acid centers, the IR spectra of H_2 were measured at -195° in IR cells or directly in a removable quartz reactor. The N_2O was absorbed at 1-50 mm Hg. The decomposition of N_2O was studied in a pulse catalytic unit at 450° or in a circulation unit at 540° at an initial N_2O pressure of 50 to 100 mm Hg with preliminary thermal vacuum treatment. The self-consistent field theory of molecular orbitals in a linear combination of atomic orbitals was then used to make nonempirical quantum chemical calculations of complexes of N_2O with Bronsted and Louis acid centers. The spectral and quantum chemical data obtained confirm that below 150°, Louis acid centers may be looked upon as centers of strong adsorption of N_2O. The N_2O molecule is activated, thus facilitating its further decomposition. Above 150°, the Louis acid centers were found to act as active centers of the reaction of the decomposition of N_2O. Figures 3; references 14: 4 Russian, 10 Western.

The Basicity of Oxide Catalysts for Oxidizing Condensation of Methane

[Article by M.Yu. Sinev, D.G. Filkova, V.Yu. Bychkov, A.A. Ukharskiy, and O.V. Krylov, Institute of Chemical Physics imeni N.N. Semenov, USSR Academy of Sciences, Moscow, and Institute of Kinetics and Catalysis, Bulgarian Academy of Sciences, Sofiya]

UDC 541.128.3:542.954.1:547.211:546.311'623'46-31:541.183

[Abstract] Oxidizing processes for producing valuable intermediate organic synthesis products are promising from the standpoint of finding ways to effect the transition to a nonpetroleum raw material. To a large degree, the problem of processing methane is reduced to selecting effective catalysts. Progress in catalyst selection in turn depends on gaining a clearer understanding of

their effect mechanism. For this reason, the authors of the study reported herein conducted a systematic investigation of the link between basicity and the catalytic properties of oxide systems in methane oxidation. Three previously described series of catalysts were selected for the study: 1) 5 mol% M_2)/MgO (M = Li, Na, K, or Cs); 2) 10 mol% M_2O/Al_2O_3; and 3) Al_2O_3 with various contents of PbO (between 1 and 20 mol%). Adsorption of CO_2 was used as a test for basicity, and the number of basic centers was determined by the thermal desorption method. Calorimetry and IR spectroscopy studies were also performed in accordance with methods described elsewhere. No correlation between catalytic and basic properties was found for the M_2O/Al_2O_3 catalysts. In the case of Pb/Al_2O_3 and M_2O/MgO, however, an adiabatic dependence between CO_2 absorption heats and the formation rate of C_2 hydrocarbons was observed. The data obtained were found to be in good agreement with the model of activation of methane with homolytic breaking of the C-H bond on an oxidizing center. Figures 4, table 1; references 28: 8 Russian, 20 Western.

Kinetics and Mechanism of the Gas-Phase Oxidation of Different Classes of C_6 Hydrocarbons on Palladium

[Article by T.M. Shaprinskaya, Institute of Physical Chemistry imeni L.V. Pisarzhevskiy, UkSSR Academy of Sciences, Kiev]

UDC 541.128.13:541

[Abstract] In a continuation of research presented in previous publications, the author of the study reported herein examined the kinetics and mechanism of gas-phase oxidation of C_6 hydrocarbons, i.e., benzene, n-hexane, hexane-1, and cyclohexane, on palladium in a gradientless Korneychuk reactor. The rate of the processes studied was measured at atmospheric pressure in the temperature range from 293 to 693 K at reaction mixture flow rates of 0.3 to 0.075 l/min and hydrocarbon concentrations in the starting hydrocarbon-air mixtures of 1.5 to 16.0 x 10^{-4} mol/l. Between 0.05 and 0.07 g palladium was applied, with the geometric surface of the palladium film ranging from 0.04 to 0.006 m^2. The main reaction products, i.e., carbon oxides, were quantitatively determined on an LKhM-8M-1 chromatograph with a katharometer (a 2-m x 3-mm column filled with tetramethyl ammonium zeolite). The effect of the following factors (which are capable of changing the course of the chain process) were studied to clarify the chain nature of the homogeneous stages by way of the example of the oxidation of benzene on palladium: packings with different chemical natures, mixing of the reaction mixture, introduction of hydrogen (in amounts from 2.5 to 15% by volume) into the reaction mixture, and changes in the dimensions of the catalyst's surface and the free

reaction spaces. The oxidation of n-hexane on palladium was examined to assess the possibility of the formation of superequilibrium concentrations of intermediate energy-rich particles. The tests were conducted at reduced pressures (32 and 100 mm Hg) in a vacuum static unit at 473-673 K with a reagent ratio of C_6H_{14}:O_2 equal to 1:9.5 (corresponding to the stoichiometry of the deep oxidation of carbon). The experiments performed led the author to conclude that the nonlinear stages of these processes play an important role in the processes overall. They experimentally established a link between the nonlinear kinetic dependences and the branched-chain nature of the heterogeneous-homogeneous stages of the reactions under consideration. Figures 3, tables 2; references 30: 1 Russian, 29 Western.

High-Temperature Transformations of Acetophenone Over Al_2O_3-MgO Catalysts

[Article by R.A. Karakhanov, V.V. Kushan, and V.D. Ryabov, Moscow Institute of Oil and Gas imeni I.M. Gubkin]

UDC 541.128.13:542.936:546.623'46-31:547.572.1

[Abstract] Acetophenone is a by-product in the production of phenol and acetone by the cumene method. In view of the practical importance of developing methods for the chemical processing of acetophenone, the authors of the study reported herein developed a catalyst consisting of Al_2O_3 and MgO for use in dehydrating acetophenone. Tests of the new catalyst were conducted at temperatures of 300 to 500° and contact times of 0.1 to 1.32 seconds with water:acetone molar ratios ranging from 7 to 26. Catalyst specimens with MgO contents ranging from 8 to 12% were examined. The best results were achieved with a catalyst containing 10% MgO. The following conditions were determined to be optimal for conducting the aforesaid catalytic reaction: temperature, 400°; molar ratio of water to acetophenone, 26; contact time, and 0.75 s. Reactions performed with these parameters yielded the following (%): phenylacetylene, 21; styrene, 14.9; and benzene and its homologues, 3.9%. Total selectivity of the catalyst with respect to phenylacetylene and styrene amounted to 90.2%. As the temperature was increased to 500° while all other conditions were kept the same, the phenylacetylene and styrene yields increased to 28.6 and 25%, respectively, but selectivity decreased to 76.3%. The proposed technology may be classified as a low-waste technology. Figure 1, table 1; reference 1 (Western).

The Link Between the Strength and Porosity of Aluminum Oxide Catalyst Carriers

[Article by M.A. Kipnis, Elektrogorod Affiliate, All-Union Scientific Research Institute of Oil Refining]

[Abstract] A large group of vapor conversion catalysts are synthesized in accordance with impregnation technology. A carrier subjected to heat treatment above 1,000° is used. This heat treatment results in sintering of the carrier and, accordingly, in an increase in its strength and a decrease in its porosity. The rate of strength increase and porosity decrease depends on the type of carrier, synthesis technology, dispersion of the starting powder, and phase composition. After briefly reviewing the existing literature on the strength-porosity correlation, the author of the study reported herein proceeds to derive an analytical form of the strength-porosity dependence for aluminum oxide carriers of vapor conversion catalysts. The effect of roasting temperature and modifiers is also examined. Although the article does not directly address the issue of the effect of additives on the strength-porosity relationship, the author does find that adding oxides is equivalent to changing the roasting temperature and that adding burn-up agents also affects the relationship. Figures 2; references 9: 6 Russian, 3 Western.

The Electrophysical Properties of GaAs Layers Grown on Nondoped Semi-Insulating GaAs Substrates From a Bismuth Melt

[Article by S.I. Krukovskiy, I.Ye. Maronchuk, and G.V. Savitskiy, Kherson Industrial Institute]

[Abstract] Epitaxial layers on substrates of semi-insulating GaAs may find wide-scale application in the technology of producing integrated circuits for different purposes. Unfortunately, the high density of point defects and dislocations in GaAs substrates make it impossible to use them as a basis for manufacturing epitaxial layers meeting the requirements of the integrated circuitry industry. In view of this fact, the authors of the study reported herein conducted experiments to establish the effect that the duration of pre-epitaxial heat treatment of semi-insulating nondoped GaAs substrates and the time and temperature conditions of the process of epitaxial growth from a solution in a bismuth melt have on the electrophysical and photoluminescence characteristics of layers of nondoped GaAs. As substrates, the authors used type AGChP-6 semi-insulating nondoped GaAs with an orientation of (100), a specific resistance of 2×10^7 Ω-cm, and a mobility of the main carriers of 5,000 cm^2/W-s. The components of the melt (Vi-0000 bismuth and polycrystalline GaAs with an electron concentration of (4 to 6) $\times 10^{15}$ cm^{-3}) were preannealed in hydrogen at 1,120 K for 16 hours. The resultant charge was used to grow GaAs layers on substrates that had been pretreated in standard etching

agent. The experiments revealed that manganese is the main uncontrolled impurity creating a compensation effect in epitaxial GaAs layers grown by the method of liquid-phase epitaxy on semi-insulating nondoped substrates. This optimal time and temperature conditions of the process were also determined. Figures 2, table 1; references 7: 6 Russian, 1 Western.

High-Temperature Halide Transport of Cerium Sulfide

[Article by A.V. Golubkov and A.V. Prokofyev, Physical Technical Institute imeni A.F. Ioffe]

[Abstract] Sulfides of rare earth elements with the composition Ln_2S_3 have attracted researchers' attention thanks to their optical properties. Materials used in optical studies must, however, meet stringent requirements: They must be perfect and transparent in the visible and infrared regions of the spectrum. Obtaining optically transparent rare earth sulfides, particularly Ce_2S_4, is a rather complicated process for several reasons. In an effort to simplify the process of producing $Ce_{inf}2S_4$, the authors of the study reported herein examined several aspects of growing optical cerium sulfide crystals by the method of chemical gas transport reactions and have presented experimental data on the growth of $Ce_{inf}2S_4$ crystals. They used the methods of equilibrium thermodynamic calculation to model the gas transport reactions entailed in the formation of $Ce_{inf}2S_4$. They calculated the equilibrium established when cerium sulfide reacts with different carriers, including iodine, bromine, hydrogen iodide, hydrogen bromide, and mixtures of each of these with hydrogen. Because hydrogen bromide turned out to be the most effective carrier, the system $Ce_{inf}2S_4$-hydrogen was examined in greater detail. Increasing the temperature was found to increase the partial pressure of cerium sulfide but did not intensify its temperature dependence. Increasing the total pressure hardly shifted the equilibrium. The authors then proceeded to study the effect of the high-temperature gas mixture on different prospective container materials (including aluminum oxide, silicon carbide, glassy carbon, and graphite). Only the carbon materials showed no visible signs of breakdown. Further analysis of the reaction of carbon and the components of the gas mixture showed that chemical transport of cerium sulfide in a carbon container using HBr as a carrier is indeed suitable for growing $Ce_{inf}2S_4$ crystals. Figure 1; references 9: 5 Russian, 4 Western.

Solid Solutions in the Systems AgGaS$_2$-GeS$_2$ and AgGaSe$_2$-GeSe$_2$

[Article by V.V. Badikov, A.G. Tyulyupa, G.S. Shevyrdyayeva, and S.G. Shenina]

UDC 541.123.2

[Abstract] Because of their low birefringence and limited transparency range, materials such as AgGaS$_2$ and AgGaSe$_2$ cannot be used to create instruments for visualization of the radiation of a CO$_2$ laser in the maximum-sensitivity range of photoreceivers. In view of this fact, the authors of the study reported herein examined the phase relationships and homogeneity regions in the systems AgGaS$_2$-GeS$_2$ and AgGaSe$_2$-GeSe$_2$ so as to assess the feasibility of using the resultant compounds as materials for visualizing infrared radiation. The test specimens were prepared by using 1, 2.5, and 5 mol.% of elements with semitransparent purity. The specimens were subjected to isothermal annealing in furnaces at 770, 830, 870, 970, 990, 1,000, 1,070, 1,080, and 1,100 K for 30 days. After annealing, the specimens were tempered in water. Differential-thermal, x-ray phase, and petrographic analysis methods were used to obtain the first-ever phase diagrams of the systems AgGaS$_2$-GeS$_2$ and AgGaSe$_2$-GeSe$_2$. On the basis of the compound AgGaGeS$_4$, the authors found the range of solid solutions Ag$_x$Ga$_x$Ge$_{1-x}$S$_2$ where $0.17 \le x$ 0.54. In the system AgGaSe$_2$-GeSe$_2$, the authors found new materials with the composition Ag$_x$Ga$_x$Ge$_{1-x}$S$_2$ (0.1 $x \le 0.4$) with the space group *Fdd*2 and nonlinear properties. Figures 2, table 1; references 6: 2 Russian, 4 Western.

The Transition of NaCl to a State With Metallike Conduction at High Pressures

[Article by A.N. Babushkin, L.Ya. Kobelev, G.V. Babushkina, and Ye.N. Yakovlev, Ural State University imeni A.M. Gorkiy]

UDC 532.111.33

[Abstract] Alkali metal halides represent the simplest ion crystals and have thus been the subject of many experimental and theoretical studies. In recent years they have aroused particular interest owing to the phase transition from an NaCl (B1)-type structure to a CsCl (B2)-type structure that is observed in most such compounds. Research is still lacking, however, on the topic of the temperature dependences of the electrical properties of alkali metal halides in general and NaCl in particular.

The authors of the study reported herein examined the temperature and baric dependences of the resistance of NaCl at pressures above 20 GPa in the temperature range from 77 to 300 K. At a temperature near 220 K, the resistance of NaCl was found to change sharply; at higher temperatures it changed in a nonmonotonic fashion. It was further discovered that the B1-to-B2 transition is accompanied by a sharp drop in resistance and that, at a pressure of 38 GPa, NaCl effects a transition into a state with a resistance temperature dependence that is characteristic of metals. The values of the transition pressure and ranges of the existence of metastable states found are in good agreement with data obtained by other researchers. Figures 3; references 18: 10 Russian, 8 Western.

Compounds Formed on the Surface of TiO$_2$-Based Ceramic Materials

[Article by L.A. Aksenova, D.V. Korolkov, Yu.P. Kostikov, and V.S. Strykanov]

UDC 666.3

[Abstract] Because of its practical importance, the concentration of impurities on the surface of solids and at the grain boundaries of polycrystalline materials has been the subject of an ever-increasing number of experimental and theoretical studies. In an entire series of ceramic materials, especially those used for electronics technology, the properties of the grain boundaries largely determine their special characteristics. The authors of the study reported herein examined the makeup of the grain boundaries of TiO$_2$-based ceramic with MgO, CaO, SrO, or PbO dopants. They also attempted to determine the main laws governing the formation of surface compounds in TiO$_2$-based systems with an alkali metal element dopant. The test specimens were prepared in accordance with conventional ceramic technology from high-purity TiO$_2$. The concentration of dopant introduced was varied from 0.01 to 10.0 mol.%. The specimens were synthesized in air at temperatures between 1,375 and 1,775 K and were cooled at a rate of about 300 K/h. The specimens' makeup was controlled by emission and x-ray fluorescent spectrum analysis. The formation of surface compounds was studied by the methods of x-ray photoelectron spectroscopy and scanning electron microscopy in accordance with procedures described elsewhere. No extraneous impurities were found to be present on the surface of the synthesized specimens within the sensitivity limits of the x-ray fluorescence spectrum analysis method used. Only in the case of the system TiO$_2$-MgO was no enrichment of the surface by the dopant observed. In all of the other cases, the concentration of dopant on the surface was much higher than the concentration introduced. The following

compounds were observed to have formed when the aforementioned dopants were added: $CaTi_4O_9$, $SrTi_4O_9$, and $PbTi_3O_7$. The M/Ti atomic ratios on the ceramic's surface was virtually independent of the annealing temperature and concentration of dopant introduced. Direct determination of the ceramic grains' surface structure by electron diffraction methods was impossible because the test specimens were dielectric. Several factors did, however, confirm the formation of compounds at the grain boundaries in the case where CaO, SrO, or PbO dopants were added. The main factor was the constancy of the makeup of the ceramic's grain boundaries in the given systems at dopant concentrations of more than 0.01 mol.%. The very high grain boundary enrichment coefficients (more than 1,000) found in the case of dopant concentrations up to 0.10 mol.% also indicates the formation of a surface compound. On the basis of their research, the authors concluded that processes of heteroepitaxy of the products of the reaction between the dopant and primary substance at the grain surface of the primary substance play a decisive role in the formation of the compounds formed. The authors further concluded that the patterns they observed during the formation of compounds on the surface of TiO_2-based ceramic materials doped with alkali earth element oxides were due to the possibility of the existence of polytitanates with a high degree of polymerization $[TiO_6]$-octahedra in the anion radicals. Figures 2, tables 2; references 13: 7 Russian, 6 Western.

The Absence of Localized Magnetic Moments in Cr-Doped TiC

[Article by D.G. Kellerman, V.S. Gorshkov, and V.A. Perelyayev, Chemistry Institute, Ural Department, USSR Academy of Sciences]

UDC 546.821'261:541.67

[Abstract] Thanks to its wide homogeneity range and simple crystalline structure, refractory titanium carbide is a convenient substance for use in research on problems of electronic structure and chemical bonding. TiC is also interesting because of its high strength characteristics, which make it suitable for use in creating hard alloys. The authors of the present article conducted a study to determine whether $Ti_{1-x}Cr_xC$ solid solutions are Pauli-type paramagnetics and whether the magnetic chromium ions in such solutions are electron localization centers. $Ti_{1-x}Cr_xC$ solid solutions ($0 \leq x \leq 0.015$) were synthesized from titanium hydride, metallic chromium, and acetylene black in a vacuum of 10^{-2} Pa at 2,100 K for 50 hours with intermediate pulverization. The solutions' magnetic susceptibility was measured by the Faraday method in the temperature range from 80 to 300 K. The authors then attempted to statistically process the data

by using a model that included a Curie-Weiss component describing a system with localized moments. The analysis conducted revealed that the said model does not adequately describe the experimental data. The authors were thus led to conclude that localization of electrons on chromium ions evidently does not occur in $Ti_{1-x}Cr_xC$ solid solutions. Figure 1, table 1; references 3: 1 Russian, 2 Western.

Ferroelectric Solid Solutions of Multicomponent Systems of Complex Oxides With High Piezoelectric Characteristics

[Article by Ye.G. Fesenko, A.Ya. Dantsinger, S.I. Dudkina, N.V. Dergunova, O.N. Razumovskaya, L.A. Reznichenko, and L.A. Shilkina, Rostov State University and Physics Scientific Research Institute]

UDC 537.226.4+537.226.86

[Abstract] High dielectric constants and high specific sensitivities are required in order for piezoceramic materials to be used effectively in low-frequency converters working in a receiver mode. High piezoelectric modulus (d_{ij}) values in the vibration exciters are also required. Because the specific sensitivity is proportional to the electromechanical coupling coefficient (K_{ij}), the materials being sought must also possess high piezoelectric parameters (i.e., high d_{ij} and K_{ij}). The authors of the study reported herein set out to find ferroelectric solid solutions of multicomponent systems of complex oxides that would have high piezoelectric characteristics. During their search, they examined compounds of the type $PbB'_{1-\alpha}B''_{1-\alpha}O_3$ (where $\alpha = 1/2$, 1/3, or 1/4 depending on the valence of B' and B'') based on $PbTiO_3$-$PbZrO_3$. Their research indicated that the highest dielectric constants and piezoelectric parameters ($\varepsilon^T_{33}/\varepsilon_0 = 5,000$ to 5,500; $K_p = 0.68$ to 0.71; and $d_{31} = 330$ to 360 pC/N) were possessed by solid solutions close to the tetragonal boundary of the morphotropic region of five-component systems when the following cations were combined in complex oxides: B'= Nb and W and B'= Zn, Mg, and Ni. Figures 2; references 8: 5 Russian, 3 Western.

A Thermodynamic Analysis of the Interaction of Selected Materials With Si and Ge Melts

[Article by A.Yu. Lvov, A.N. Pronchatov, A.O. Markov, and S.V. Yankov, Institute of the Chemistry of Highly Pure Substances, USSR Academy of Sciences, Nizhniy Novgorod]

UDC 545.28:666.762

[Abstract] The contaminating effect of the container during final purification of germanium and silicon is currently the main factor preventing production of purer forms of these materials, which are so vital to semiconductor technology. The contamination of Si and Ge monocrystals due to the quartz glass on which they are grown is significant. When it comes into contact with liquid Si, quartz glass crystallizes rapidly, and the product loses its initial shape. In view of the urgent need to find alternative materials for use in growing Si and Ge monocrystals, the authors of the study reported herein undertook a thermodynamic analysis of the reaction when selected refractory oxides, carbides, nitrides, and carbon come into contact with Ge and Si melts. The authors determined the equilibrium composition in silicon melt-growing container material at 1,690 K for 14 different materials (TiN, BeO, ZrO_2, Si_3N_4, SiO_2, AlN, Al_2O_3, ZrC, TiC, SiC, BN, graphite, WC, and B_4C) (assuming the formation of ideal solutions). They also determined the equilibrium composition of Ge-container material melts (again assuming the formation of ideal solutions) consisting of Ge and the same 14 materials examined in relation to Si. On the basis of their thermodynamic analyses, the authors recommended that carbon-based materials be used when growing Ge monocrystals. They were unable to recommend any one material for the deep purification of Si. Many of the materials that they tested were found to be sources of undesirable impurities in the Si melt (oxygen, nitrogen, aluminum, and/or transition metal impurities). They were, however, able to state that high-purity silicon carbide holds promise as a prospective container material for use in growing Si monocrystals inasmuch as it is not a source of electroactive impurities in the resultant semiconductor. They leave final selection of a material up to the individual and state that this selection should be based on a study of the kinetics of the contamination of the melt by the main components and impurities of the candidate growth container materials. Tables 5; references 16: 6 Russian, 10 Western.

Estimating the Inleakage of Impurities From Air Into High-Purity Gas Transported Via Polymer Pipelines

[Article by V.I. Faynshteyn and N.V. Pavlov, All-Union Scientific-Research Institute of Cryogenic Machine Building, Moscow Oblast]

UDC 66.073.3:66.074.3

[Abstract] Various sectors of industry (nuclear, electronic, chemical, etc.) rely on high- and ultrahigh-purity gases. In view of the need to retain the purity of pipeline-transported gases up to their final destination, the authors of the study reported herein examined the process of the inleakage of air impurities into high-purity argon transported via polymer pipelines. They conducted their experiments at room temperature (20°C) with polymer pipelines made of fluoroplast-4, high-pressure polyethylene (modified carbon blacks), and polyvinyl acetate. The pipelines used ranged from 0.4 to 12.7 m in length and 0.006 to 0.08 m in diameter. They all had a wall thickness of 1 mm. The argon transport speed was varied from 0.066 to 0.60 m/s. According to the authors' calculations, the three materials studied were found to have the following permeability coefficients (in [(cm^3 x cm)/s x cm^2 x Pa)] x 10^{14}): high-pressure polyethylene, 6.5 +/- 0.2 for O_2 and 296 +/- 12 for H_2O; polyvinyl acetate, 26.3 +/- 0.4 for O_2 and 7,770 +/- for H_2O; and fluoroplast-4, 71.4 +/- for O_2 and 264 +/- 14 for H_2O. The differences between the values found by the authors and those obtained by other researchers were attributed to differences between the test materials used (specifically, differences between domestic and foreign materials). The authors verified their own results by conducting a check experiment using imported fluoroplast. The permeability coefficients obtained in that experiment virtually coincided with data reported in the literature. Figures 2, tables 2; references 7: 4 Russian, 3 Western.

Ecologically Clean and No-Waste Technology and Equipment for Deep Liquid-Phase Cleaning of Silicon Plates and Structures

[Article by S.O. Izidinov, V.I. Gaponenko, P.P. Shkarmutin (deceased), A.M. Krasnobayev, and R.I. Rybak, All-Union Electrical Engineering Institute imeni V.I. Lenin, Moscow]

UDC 546.28.121

[Abstract] The modern semiconductor instrument industry could not function without using a broad class of high-purity materials. In view of the high cost and importance of semiconductor materials such as silicon, the authors of the study reported herein set out to develop an ecologically clean no-waste technology and equipment for deep liquid-phase cleaning of silicon plates and structures. After reviewing the literature on existing cleaning technologies and equipment, the authors identified five factors essential to effective deep cleaning. In essence, these factors are as follows: 1) coordination complexes of nitrile and alcohol molecules intensify a system's desorption; 2) alcohol molecules reduce the possibility of readsorption of cations from the near-surface layer at the interface; 3) nitrile-alcohol coordination complexes not only facilitate complete desorption but also intensity the alkoxylation reaction; 4) the azeotropic system alcohol-nitrile cleanses the surface of impurities in the form of soluble alcoholates as a result

of an alcoholysis process; and 5) acetonitrile is an excellent solvent for oils, lacquers, fats, cellulose ethers, many synthetic polymers, and inorganic salts and is a good extractive reagent for separating fatty acids from oils and animal fats. Working with these factors in mind, the authors designed a prototype unit for deep cleaning of silicon plates and structures in a continuously recoverable organic azeotropic mixture. The unit consists of two modules. In the first, condensate is distilled, prepared, and metered. The second is the actual process module. It may be connected with other standard modules in a Lada-Elektronika system in a liquid-phase cleaning process line. Tests demonstrated that a module holding a volume of 50 liters of mixture can operate continuously for at least 1.5-2 months, during which time it can complete 1,500 to 2,000 cycles in a two-shift operation. The new equipment produces less waste than conventional equipment. An additional advantage of the new equipment is that it is capable of cleaning the faces of semiconductor structures. The new equipment has successfully passed tests at the Preobrazovatel ZPO [not further identified]: the amount of impurities separated out of the silicon and remaining in the evaporator was two- to threefold higher than the amount resulting from the conventional procedure, and laser mass spectrometry studies revealed that silicon cleaned by using the new technology and equipment had its amounts of Fe, Cr, Al, Mg, Ca, Na, etc., impurities reduced by a factor of 3 to 15 versus specimens cleaned by the conventional technology. Figure 1; references 17: 14 Russian, 3 Western.

Using a Stabilized ZrO_2-Based Solid-Electrolyte Cell To Concentrate Permanent Gas Impurities in Oxygen

[Article by V.A. Krylov, S.G. Krasotskiy, A.V. Sarkisov, A.D. Neuymin, and V.A. Arzhannikov, Institute of the Chemistry of High-Purity Substances, USSR Academy of Sciences, Nizhniy Novgorod]

UDC 543.54:64

[Abstract] Producing the high-purity oxygen required to synthesize the high-purity oxides used in fiber optics and microelectronics entails developing and perfecting methods of analyzing it. The preferred method of determining impurities in oxygen is gas chromatography. It is distinguished by its higher sensitivity and relatively simple equipment requirements. Gas chromatography has been successfully used to determine neon, argon, nitrogen, and carbon oxide impurities in oxygen in quantities ranging from 10^{-4} to 10^{-5} molecular percent. These detection limits are not adequate in all cases, however. Moreover, the need for regular replacement of the reactor and the length of time required to prepare the reactor significantly reduce the productivity of gas chromatographic analysis. For these reasons, the authors of

the study reported herein examined the prospects of using a stabilized zirconium dioxide-based solid-electrolyte cell for use in concentrating permanent gas impurities in oxygen. The authors designed their new method on the basis of a Tsvet-500 chromatograph equipped with a helium ionization detector. Grade B (TU 51-940-80) helium was used as the carrier gas. The gas was fed at a flow rate of 50 ml/min. A drying and cryoadsorption cleaning system was used to achieve gas with the required purity. The background current of the detector (which operated in a saturation current mode) amounted to 3×10^{-9} A at an electrode voltage of 55 V. The impurities were separated on a chromatographic column 2 mm in diameter and 70 mm long that was filled with CaEt molecular sieves (fraction, 0.1 to 1.6 mm). The column's effectiveness with respect to oxygen impurities amounted to 700 theoretical plates, and the column was thermostatted at 70 +/- 0.1°C. The specimen was concentrated in an electrochemical cell made of ZiO_2 stabilized by CaO. The cell was manufactured in the form of a flowthrough ceramic test tube with silver electrodes. The working temperature amounted to 820 +/- 5°C, and atmospheric air served as the external medium. Samples for the oxygen analysis were taken from the tank with the analysis gas or from the flowthrough glass ampule. The ampule was prepared for the gas sampling by cleaning the inner surface with a glow discharge and subsequently rinsing it with purified He, followed by evacuation to 10-20 Pa. The oxygen was pumped out to a residual pressure of 10^{-7} MPa. The amount of oxygen removed when concentrating the impurities for determination was controlled by the current passing through the solid-electrolyte cell. The method developed proved capable of determining impurities in amounts as low as 10^{-5} to 10^{-6} molecular percent in a 50-ml specimen. The new method was found to have a total determination error of less than 10%. Figures 4, tables 3; references 12: 9 Russian, 3 Western.

Extraction Atomic Emission Analysis of Alkyl Derivatives of Mercury

[Article by O.V. Shuvayeva, I.G. Yudelevich, Yu.I. Amosov, and N.P. Ryazantseva, Inorganic Chemistry Institute, Siberian Department, USSR Academy of Sciences]

UDC 543.064+547.254

[Abstract] The development of high-sensitivity multielement methods of analyzing the impurities present in organometallic compounds is essential if organometallic mercury compounds are to be suitable for use in gas-phase epitaxy. Others have managed to detect 10 impurity elements in organometallic compounds at a level of 3×10^{-4} to 2×10^{-7} percent by weight. The authors of the study reported herein worked to extend this detection

range. They developed a method for chemical atomic emission determination of 21 impurity elements (Al, Ba, Ca, Cd, Cr, Cu, Fe, In, Ga, Mg, Mn, Mo, Ni, P, Pb, Sn, Sb, Te, Ti, V, Zn) in dialkyl mercury. The method entailed extraction of the base by dioctylsulfide after mineralization. An ISP-28 quartz spectrograph with a two-lens slit illumination system (a direct current of 10 A, slit width of 10 μm, and exposure time of 8 seconds) was used for atomic emission analysis of the concentrate. The "add-find" method was used to verify the method's effectiveness in determining four elements (Cd, Te, Pb, Sn). The proposed method resulted in a detection limit ranging from 5×10^{-8} to 1×10^{-5}. The new method was recommended for use in determining the impurity profile of different alkyl derivatives of mercury (symmetrical and asymmetrical). The authors caution, however, that each compound will require different mineralization conditions to be selected with consideration given to the reactivity and makeup of the reaction by-products. Tables 3; references 8: 7 Russian, 1 Western.

Synthesis of Fluorozirconate Glasses With Reduced Oxygen Content

[Article by M.N. Brekhovskikh, V.A. Fedorov, V.S. Shiryayev, and M.F. Churbanov, Institute of General and Inorganic Chemistry imeni N.S. Kurnakov, USSR Academy of Sciences, Moscow, and Institute of the Chemistry of High-Purity Substances, USSR Academy of Sciences, Nizhniy Novgorod]

UDC 546.161

[Abstract] Thanks to their broad transparency range (extending from 0.3 to 8 μm) and their potentially low optical losses in lightguides, glasses based on heavy metal fluorides have attracted increasing interest. Their theoretically estimated minimal level of natural optical losses amounts to 0.01 dB/km. Estimates indicate that the presence of 1 ppm hydroxide ions in such glass may result in an attenuation of up to 10^{+4} dB/km at a wavelength of 2.9 μm. Oxygen impurities in the form of oxide bridges or metal oxides may, however, cause such glass to crystallize. Despite the significant progress that has been made in the area of purifying the starting components used when synthesizing glass, the problem of impurities in fluoride lightguides still remains unsolved. Additional fluorination of the initial components in a fluorinating atmosphere is currently used to eliminate oxygen-containing impurities in fluoride glasses. The degree to which the charge is cleansed of oxygen as a result of the substitution reactions remains inadequate, however. The authors of the study reported herein have therefore proposed a method of additional fluorination of the charge with volatile inorganic fluorine oxidizing agents, i.e., xenon, chlorine, and bromine fluorides. Control fluorozirconate glass specimens were produced by presintering the charge components at 500-550°C for 1 to 2 hours in an argon atmosphere, melting at 900 to 950°C for half an hour, and cooling in air. The resultant specimens all had an oxygen content ranging from 0.1 to 0.3 percent by weight. Test specimens were then produced by using the proposed method. These specimens, which were produced in a procedure that entailed pretreatment of the charge by either xenon difluoride, bromine trifluoride, or chlorine trifluoride all had oxygen contents not exceeding 3×10^{-3} percent by weight. Laser ultramicroscopy studies were performed to compare the optical uniformity of the three types of test specimens with that of the control specimens. XeF_2 was determined to be the most effective fluorinating agent for processing charge; the degree of crystallinity obtained when it was used amounted to 2×10^{-9} with a particle concentration of 3×10^{-6} cm^{-3}. Glasses treated with bromine trifluoride turned out to have wide degree-of-crystallinity and particle concentration values. Using chlorine trifluoride was found to result in strong scattering of radiation on particles of submicronic size. Figures 2, table 1; references 9: 6 Russian, 3 Western.

Optical Fiber IR Radiometer for Medical Diagnosis

[Article by G.G. Devtatykh, V.A. Ivantsov, V.S. Lebedev, V.V. Lychev, I.Ya. Orlov, V.G. Plotnichenko, I.V. Skripachev, G.Ye. Snopatin, V.M. Solovyev, and M.F. Churbanov, Institute of the Chemistry of High-Purity Substances, USSR Academy of Sciences, and Nizhgorod State University]

UDC 546.19'23:54-161.621.391.029.7

[Abstract] Various stable changes in a person's temperature field frequently precede clinical symptoms of a pathologic process and thus serve as indicators for early diagnosis. Unlike x-ray computer tomography, the radiometric method makes it possible to diagnose a pathologic process before tissue changes have occurred. In view of the promise of the radiometric method of diagnosis in such branches of medicine as oncology, inflammatory disease, and cardiovascular disease, the authors of the study reported herein developed an optical fiber infrared radiometer for use in medical diagnosis. From fiber lightguides of the glass-polymer ($As_{35}Se_{65}$-fluoroplast F-42) type, they manufactured an irregular braid consisting of 180 individual fibers. The braid was used as a telescope in an IR radiometer developed for purposes of medical diagnosis. The IR radiometer was used under clinical conditions to check the temperature of patients' eyeballs after they had undergone cataract removal and surgical glaucoma treatment. Tests conducted on the new device demonstrated the effectiveness of an optical fiber IR radiometer in thermometric diagnosis. Because of its protection

against external electromagnetic microwave fields, the optical fiber IR radiometer may, according to the authors, be used in monitoring the hyperthermia process during cancer treatment. Because of the high reflection factor of chalcogenide glasses, about 40% of the intensity of the IR radiation received and transmitted by the braid is lost upon introduction and withdrawal. The authors state that the braid's efficiency and, consequently, the sensitivity of the IR radiometer may be increased by applying an antireflective coating onto its faces. Figures 3; references 8: 5 Russian, 3 Western.

The Problem of Waste Recovery When Cleaning Potash to the Level Required for Optical Glassmaking

[Article by L.A. Nesterova, A.V. Bromberg (deceased), Z.P. Bystrova, I.N. Orlova, V.G. Sevastyanov, and A.N. Vasnev, All-Union Scientific Research Institute of Chemical Reagents and Superfine Chemicals, Moscow]

UDC 537.311:546

[Abstract] The problems of waste recovery, while important throughout industry, become especially important when speaking of high-capacity production processes such as the production of chemically pure calcium carbonate for use in optical glassmaking. After summarizing the research that has already been done in this area, the authors of the study reported herein set about solving the problem of recovering hydrocarbonate wastes as it applies to the technology of processing potash into chemically pure calcium carbonate for optical glassmaking by the carbonization method. To do so, they studied the behavior of dye and anionic impurities during the process of processing potash by the carbonization method when several alternative methods were used to recover the mother liquor. Their tests led them to conclude that recovery of hydrocarbonate solutions after preliminary decarbonization by boiling does not appear promising under commercial conditions when producing a product with a limited content of dying elements. Recycling the mother liquors and process waters plus salting out the hydrocarbonate by potash and subsequently using it in the very same process not only provides a highly stable product quality but also affords a number of technical and economic advantages over the other alternatives considered. Because there is no lengthy (15 to 18 hours) and corrosive decarbonization stage, the power consumption and labor input required for the process are reduced, and there is no need to use large-capacity equipment or, accordingly, large production sites (which are in short supply at a number of plants). The authors state that the process flow they describe makes it possible to set up production of calcium carbon that has a chemical purity suitable for optical glassmaking by using inexpensive and accessible domestic raw material. Figure 1, tables 3; references 5 (Russian).

Oxygen Nonstoichiometry of $YBa_2Cu_3O_x$

[Article by G.D. Nipan, V.P. Sanygin, A.M. Kvardakov, V.V. Volkov, and A.V. Filatov, Institute of General and Inorganic Chemistry imeni N.S. Kurnakov, USSR Academy of Sciences]

UDC 539.7

[Abstract] The question of the qualitative interconnection between the oxygen nonstoichiometry of high-temperature superconductors and their structure and electrical and magnetic properties remains open, as does the question of the thermal stability of their superconducting phases. In an effort to shed further light on these problems, the authors of the study reported herein examined the oxygen nonstoichiometry of $YBa_2Cu_3O_x$. To avoid metal content determination errors associated with the inherent nonstoichiometry when high-temperature superconductors are synthesized from oxides with a high hygroscopicity and errors associated with the formation of crystal hydrates during synthesis from salts, the authors synthesized the test high-temperature superconductors from the metals Y, Ba, and Cu. Their selection of this method was dictated by the fact that the method makes it possible to estimate the absolute oxygen content as the difference between the mass of the synthesized $YBa_2Cu_3O_x$ polycrystals and the mass of the pure metals. The methods of electron probe microanalysis, iodometric titration, and x-ray fluorescence analysis were used to determine the element and phase makeup of the specimens, and the method of four-probe measurement of electric conduction was used together with a vibration magnetometer to measure their superconductivity properties. The method of static tensimetry with a spoon-type quartz zero-pressure gauge was used to study the ceramic materials' oxygen nonstoichiometry in the temperature range form 700 to 1,320 K and in the pressure range from 0.1 to 100 kPa. The temperature dependence of the oxygen index did not change by more than 0.01 when the initial absolute oxygen index was varied from 6.0 to 6.6. The temperature dependence of the oxygen index in the temperature interval from 700 to 1,170 K did not exceed 13 K. The point of inflection occurred at a temperature of about 870 K, which is in agreement with the polymorphous transition in $YBa_2Cu_3O_x$ discussed elsewhere. When an initial oxygen index of 6.60 is assumed, a rhombic Y-Ba modification is found to occur at oxygen indices of 6.6-6.3 (up to 870 K), and a tetragonal modification is found to occur at 6.3-6.05 (from 870 to 1,170 K). The iodometric analysis results confirm a loss of Cu during synthesis. Figures 3; references 8: 4 Russian, 4 Western.

Synthesis of CdSc₂O₄ Compounds

[Article by A.K. Vazhnov, Moscow Institute of Fine Chemical Technology imeni M.V. Lomonosov]

UDC 541.123.2

[Abstract] The system $CdO-Sc_2O_3$ is the least studied of the oxide systems containing cadmium and group III elements. Information about it is limited primarily to the statement of the existence of the complex oxide $CdSc_2O_4$. The authors of the study reported herein present experimental data that fill part of this knowledge gap. In the first phase of their experiments, they synthesized $CdSc_2O_4$ from Sc_2O_3 and CdO according to ceramic technology in the temperature interval from 850 to 950°C ($\tau = 20$ hours) and at 1,050°C ($\tau = 5$ hours). The resultant suspension was pressed into a tablet and annealed in air in a corundum crucible at low temperatures. The annealing temperature was then increased to 1,050°C, and the specimen was waltzed into platinum foil. In the culminating series of experiments, the authors used the method of thermal decomposition of coprecipitated hydroxides of cadmium and scandium to produce $CdSc_2O_4$. X-ray fluorescence analysis was used to monitor the occurrence of the reaction. The compound was confirmed to be a spinel from the standpoint of structural type (a = 9.00 angstroms), and the nature of its melting was established. A chemical analysis conducted on the synthesized $CdSc_2O_4$ produced the following results (in mol%): CdO, 49.95; Sc_2O_3, 50.05. Table 1; references 4: 1 Russian, 3 Western.

The Reaction of (NH₄)₂ZrF₆ and (NH₄)₃ZrF₇ With Nitrates of Strontium and Lead

[Article by G.F. Krysenko, Ye.I. Melnichenko, D.G. Epov, and S.A. Polishchuk, Chemistry Institute, Far Eastern Department, USSR Academy of Sciences, Vladivostok]

UDC 546.161'831'431+543.226

[Abstract] In an attempt to extend the results of previous studies of the reactions of ammonium fluorozirconates with barium nitrate, the authors of the study reported herein examined the reactions of $(NH_4)_2ZrF_6$ and $(NH_4)_3ZrF_7$ with nitrates of strontium and lead. As starting materials they used chemically pure-grade strontium and lead nitrates, high-purity acetone, high-purity 45% hydrofluoric acid, and saturated solutions of $(NH_4)_2ZrF_6$ and $(NH_4)_3ZrF_7$ corresponding to concentrations of 0.41 and 0.36 mol/l, respectively. The synthesis was performed in accordance with a method published elsewhere. The reactions between synthesized compounds and Sr and Pb nitrates were studied by chemical, x-ray phase, and thermogravimetric analyses and IR spectroscopy. The studies performed confirmed the formation of anhydrous hexa- and octafluorozirconates of strontium and lead in the form of the the binary salts $MZrF_6·0.5NH_4F$ and $M_2ZrF_8·0.5NH_4F$. At temperatures between 315 and 430°C, these compounds break down into the respective hexa- and octafluorozirconates. The effect of hydrofluoric acid on the makeup of lead fluorozirconates was also studied. It was discovered that Pb_5ZrF_{14} may be obtained in a high yield from a solution of any ammonium fluorozirconate in the presence of hydrofluoric acid. This study marks the first time that Sr_5ZrF_{14} was isolated from solutions of $(NH_4)_3ZrF_7$. Figures 2, table 1; references 6: 4 Russian, 2 Western.

The Reaction of Silicon With Lithium and Potassium Hydroxides

[Article by B.F. Dmitruk and N.N. Babich, Institute of General and Inorganic Chemistry, UkSSR Academy of Sciences]

UDC 541.124:546.28

[Abstract] Silicon reacts in one and the same way with solutions of sodium hydroxides and potassium hydroxides: it forms metasilicates and gives off hydrogen. In an effort to shed more light on the sequence of the aforesaid reactions and the makeup of the reaction products, the authors of the study reported herein used the methods of x-ray fluorescence analysis and derivative differential thermal analysis to study the reactions occurring in MOH-Si mixtures with molar component ratios ranging from 2:1 to 4:1. They used silicon of semiconductor purity, analytic-grade potassium hydroxide, and chemically pure MOH. The latter was carefully dehydrated at 550-600°C for 1.5 to 2 hours. The different MOH-Si (M = Li, K) mixtures were prepared in a dry chamber. The processes occurring in the mixtures were studied on an OD-102 derivative differential thermal analyzer at a heating rate of 3 to 15 degrees per minute in an atmosphere of air, oxygen, and conventional and moistened argon. The participation of oxygen and water vapors in the formation of potassium silicates was established. The compounds with the highest oxygen contents obtained in these systems were those with the formulas $K_6Si_2O_7$ and Li_4SiO_4. The formation of a high-temperature form of K_2O was established in the reaction of silicon with potassium hydroxide in an inert atmosphere. The authors propose a schema of the occurrence of the

reactions entailing the evolution of hydrogen. Figures 3; references 5: 3 Russian, 2 Western.

The Reaction of Hydrogen Halides With Silanol and Amine Groups on a Silica Surface

[Article by V.M. Gunko, Ye.F. Voronin, and A.A. Chuyko, Institute of Surface Chemistry, UkSSR Academy of Sciences, Kiev]

UDC 541.183

[Abstract] In an attempt to address the need for detailed study of the effect of various factors on the chemisorption of hydrogen halides on a silica surface, the authors of the study reported herein performed a quantum chemical analysis of the factors that determine the nature of the reaction of anhydrous gaseous hydrogen halides with a silica surface containing isolated $\equiv$Si-OH and $\equiv$Si-NH$_2$ groups. The authors succeed in establishing that the differences in the reaction of hydrogen halides with surface silane and amine groups is dictated not so much by steric obstacles and by the total heat effect as by the nature of the $\equiv$SiX...HHal, $\equiv$Si [left arrow] Hal, and $\equiv$Si-Hal bonds in the sorption complexes and by the distinctive features of the H$^+$ transfers in the transition states. In the case of HF, these differences play a minimal role owing to the very low polarizability and maximal strength of the H-Hal bond and to the possibility of the formation of a metastable four-center intermediate. In the remaining hydrogen halides, the four-center complexes correspond solely to the transition state. Figures 3, tables 3; references 13: 9 Russian, 4 Western.

BaBiO$_y$ Phase Transformations

[Article by L.A. Klinkova, M.V. Filatov, N.V. Barkovskiy, and D.Ye. Batova, Institute of Solid-State Physics, USSR Academy of Sciences]

UDC 669.018.537.312.62

[Abstract] The discovery of superconductivity in Ba$_x$Pb$_{1-x}$BiO$_y$ and K$_x$Ba$_{1-x}$BiO$_y$ has revived interest in barium monobismuthate. In view of this fact, the authors of the study reported herein synthesized a single-phase specimen of the makeup BaBiO$_{2.31}$ that does not contain Bi^{+5} ions or a tetragon crystallized in its structure (a = 4.39 and c = 4.53 angstroms). Thermal, x-ray spectral, and x-ray phase analyses performed on the test specimens indicated that the oxygen index of barium monobismuthate ranges from 2.31 to 2.80 during the process of oxygen annealing. Bi^{+5} ions are formed during the oxidation process in the amount of 42.6% of the total bismuth content by mass. The studies also established that the phase transition to a cubic structure (a = 4.34 angstroms) that occurs at 450°C is characterized by the maximal oxygen index values and maximum Bi^{+5} ion content. Two cubic phases were found to coexist in the temperature interval from 450 to 780°C. One remains stable in an oxidizing atmosphere until the melting point, whereas the other undergoes a structural transition at 780°C. Within this temperature range, the Bi^{+5} ion content fluctuates from 37.6 to 42.6% of the total amount of bismuth. The presence of bismuth ions with a valence of less than three in the test specimens is hypothesized. Figures 4, tables 4; references 16: 5 Russian, 9 Western.

Ba$_2$Bi$_3$O$_y$ and BaBi$_2$O$_y$ Synthesis and Structural Phase Transformations

[Article by L.A. Klinkova, M.V. Filatova, N.V. Barkovskiy, D.Ye. Batova, and V.I. Kushnir, Institute of Solid-State Physics, USSR Academy of Sciences]

UDC 669.018:537.312.62

[Abstract] Previous studies have established that the change in the oxygen index y in Ba$_2$Bi$_3$O$_y$ and BaBi$_2$O$_y$ during annealing in oxygen at 450 to 1,000°C occurs in accordance with their content of Bi^{+5} ions. The literature on the aforesaid compounds is not, however, unanimous as to its conclusions regarding the structural phase transformations of similar compounds with different molecular percentages of BaO. In view of this fact, the authors of the study reported herein selected two compounds containing 50 and 57.1 mol% BaO. These compounds correspond to the formal compositions BaBi$_2$O$_y$ and Ba$_2$Bi$_3$O$_y$, respectively. These compounds were selected for study because they are the foundation of superconductive compounds of the type K$_x$Ba$_{1-x}$BiO$_y$. The test compounds were studied in an argon and oxygen atmospheres in the temperature range from 450 to 1,100°C. Analyses of the test compounds indicated that, upon melting in argon, the phases Ba$_2$Bi$_3$O$_{5.98}$ and BaBi$_2$O$_{3.70}$ crystallize into tetragonal (a = 4.34 and c = 4.50 angstroms) and orthorhombic (a = 4.35, b = 4.41, and c = 4.50 angstroms), respectively, and that they do not contain Bi^{+5} ions. In an oxygen atmosphere, the phases Ba$_2$Bi$_3$O$_{6.08}$ and BaBi$_2$O$_{4.02}$ undergo a structural transition into a cube and are characterized by a lattice parameter of 4.36 angstroms in both cases. The content of Bi^{+5} ions in these phases amounts to 24.6 and 15.3%, respectively. Figures 4, tables 5; references 5: 2 Russian, 3 Western.

Phase Ratios in the Polythermal Section Y₂BaCuO₅-CuO of the Ternary System Y₂O₃-BaO-CuO

[Article by G.A. Mkikrticheva, V.I. Shitova, L.Yu. Grabovenko, D.P. Romanov, and R.G. Grebenshchikov, Institute of Silicate Chemistry imeni I.V. Grebenshchikov, USSR Academy of Sciences]

UDC 541.123+546.562+537.312.62

[Abstract] The information that has been obtained to date about particular sections of the system Y₂O₃-BaO-CuO is not complete enough to construct phase diagrams of this ternary system. For this reason, the authors of the study reported herein examined phase equilibria in the polythermal cross section Y₂BaCuO₅-CuO. The methods of annealing and hardening and x-ray phase, crystal optic, and differential thermal analyses [DTA] were used to plot the phase diagrams. The test specimens were produced by solid-phase synthesis from mixtures of the oxides Y₂O₃, BaO₂, and CuO at 880 to 930°. The method used to study the sections is analogous to one published in several other works. The cross section studied was determined to be eutectic-perieutectic in type and to be characterized by complex phase interrelationships in the high-temperature part of the section. Because chemical compounds containing bivalent copper are unstable at high temperatures, two versions of the polythermal section of this cross section were plotted. One was based on data from the annealing, and the other was based on DTA. In the diagram based on the DTA results, the temperature boundaries of the existence of the phase fields were elevated when compared with those in the diagrams based on the annealing and hardening results. Figures 3; references 13: 5 Russian, 8 Western.

The Possibility of Producing Superconductive Cu-Containing Phases Based on Layered Bismuth Oxohalides

[Article by L.N. Kholodkovskaya, V.A. Dolgikh, and B.A. Popovkin, Moscow State University imeni M.V. Lomonosov]

UDC 546.87.42.21.141'131

[Abstract] Of all the recently discovered high-temperature superconductors, Bi(Tl)-Cu oxide compound-based materials have the highest superconductivity temperatures (T_c). From a structural standpoint they are close to Bi₂O₂X Aurivillius phases, where X represents perovskite-like layers with the general formula A_{n-1}B_nO_y (n = 1 to 5). There is another group of layered compounds that are described by the same general formula but for which the structural element X has a zero chemical nature; for example, X may represent halogens. A recent publication has demonstrated the possibility of producing layered substances based on the alternation of Bi₂O₃ layers separated by layers of halogen atoms and perovskite-like layers, where Ti, Nb, W, etc., can act as the cation B. This class of compounds has been termed Bipox (where Bi stands for bismuth, p for perovskite, and ox for oxide). The authors of the study reported herein attempted to obtain Bipox-type compounds in which copper acts as the cation B in the perovskite layer. In other words, they tried to synthesize compounds with structures close to the familiar high-temperature superconducting phases 2212 and 2223 in which the Bi₂O₂ layers located between the two Sr-O layers alternated not only with Ca_{n-1}Cu_nO_y blocks but also with layers of chlorine or bromine atoms. As starting reagents they used ultrapure Bi₂O₃ and CuO, pure CuCl₂ and CuBr₂, and pure SrO and CaO. They studied the reaction of BiOX (X = Cl, Br) with mixtures of bismuth, strontium, potassium, and copper oxides as well as the reaction of a prepared 2212 phase with CuX₂ (X = Cl, Br). BiSrO₂X (X = Cl, Br) was discovered to be the reaction product in all cases. No new phases were formed under the conditions of the experiment reported. Table 1; references 6: 5 Russian, 1 Western.

Nuclear Resonance in High-Temperature Superconductors

[Article by A.A. Gippius, E.A. Kravchenko, and V.V. Moshchalkov,

UDC 541.67+543.42.23

[Abstract] This review discusses the results of research on the phenomenon of high-temperature superconductivity in ceramics and monocrystals of various metal oxide systems produced by using the methods of nuclear magnetic resonance [NMR] and nuclear quadrupole resonance [NQR]. The review concentrates on research published in the period 1987-1989. The topics of crystal chemistry, the charge states of atoms, and the spin dynamics of electrons in metal oxide compounds in both the normal and superconductive states are examined. Specifically, the first section of this four-section review discusses NQR studies of [63,65]Cu in YBa₂Cu₃O_x [1-2-3 superconductors] with various oxygen contents. Section 2 covers the following aspects of NMR and relaxation in 1-2-3 superconductors: NMR spectra of copper in YBa₂Cu₃O_x compounds, the Knight shift in copper lines

in 1-2-3 compounds, spin-lattice relaxation of ^{63}Cu nuclei in the system $YBa_2Cu_3O_x$, relaxation in the normal state $(T > T_c)$, and the superconductive state. The third section deals with NMR studies of ^{17}O nuclei in 1-2-3 compounds and NMR studies of ^{89}Y in 1-2-3 compounds. The fourth and final section covers the distinctive features of the NQR spectra of ^{139}La in La-Sr(Ba)-Cu-O and the temperature dependence of spin-lattice relaxation. Figures 16, tables 7; references 65: 8 Russian, 57 Western.

Casting Elastomers: Oligoether-Based Segmented Ureathane-Urea Polymers

917M0127A Moscow KAUCHUK I REZINA in Russian No 2, Feb 91 pp 11-13

[Article by S. M. Yakzhina, T. A. Yagfarova, I. L. Gerasimova and B.Ya. Teytelbaum]

UDC 678.664

[Abstract] Thermomechanical studies were performed on oligooxypropylenediol-based urethane-urea polymers to assess their suitability for casting processes. The results demonstrated that elastomers based on 2000 MW oligoether and 22.2-36.9% by wt. of rigid segments have a wide working range, as shown by T_g values ranging from -57°C to free-flow temperatures approaching 233°C. Typically, such polymers have Shore A hardness of 83 units, tensile strength at break of 20.0 MPa, elongation at break of 560%, and residual deformation of 12%. Figures 2; tables 3; references 10: 5 Russian, 5 Western.

Improved Stress-Strain Properties of Rubber in Finished Products

917M0127B Moscow KAUCHUK I REZINA in Russian No 2, Feb 91 pp 18-21

[Article by Yu. S. Zuyev]

UDC 678.01:539.4

[Abstract] An analysis was conducted on stress factors affecting in finished rubber products to assess the relationship between laboratory testing and performance under actual use. Studies conducted with tires, conveyor belts and various valves revealed considerable discrepancies between tensile strength as determined under controlled conditions in the laboratory and actual performance. This was attributed to the differences between the two situations and the myriad of other forces to which an object is subjected under actual operating conditions. Fibnally, the data showed that the tensile strength of rubber can be improved in two fundamental ways. One involves manipulating the molecular structure of rubber to impart to it the desired mechanical properties. The other approach involves modifations in design and fabrication of the products to take advantage of the physicochemical and mechanical characteristics of the elastomers to their best advantage. References 34 (Russian).

Impact Damping by Rubber Absorbers

917M0127C Moscow KAUCHUK I REZINA in Russian No 2, Feb 91 pp 26-27

[Article by V. G. Maslennikov and N. V. Kalmykov]

UDC 618.4.06:62-788.2.620.178.167

[Abstract] Nitrile-butadiene rubber (NBR) cylinders, with a relative hardness of 75-80 units, were employed in impact damping studies to expand the fund of fundamental data on the use of resins in shock absorption. The results showed that in the case of BNR almost 90% of the initial impact energy is dissipated due to the 'energy capacity' of BNR which is on the order of 12 J/cm^3. Accordingly, BNR was shown to exceed the damping capacity of most other viscoelastic materials and appears to merit further assessment for commercial applications. Figures 4; references 3 (Russian).

Cross-Sectional Profile and Heat Buildup in Large Tires

917M0127D Moscow KAUCHUK I REZINA in Russian No 2, Feb 91 pp 28-29

[Article by A. G. Smirnov, A. M. Polonov and L. B. Nikitina]

UDC 678.4.065.62.181.2:658.512.2:536.495

[Abstract] The relationship between heat buildup and large tire profile was analyzed in order to define parameters that might lead to improved tire designs. Preliminary studies relating heat buildup to height to width ratio (H/W) were conducted for 17.5-25, 18.00-25, 20.5-25, 26.5-25 tires, among others, bearing loads of 80 and 100 kN and tire pressure of 0.6 MPa. The data were used to derive mathematical equations relating maximum allowable temperature ($<$/= 100°C), load, and tire pressure in relation to recommended H/W. In general, the data indicate that H/W ratios should be limited to $<$ 0.75 to avoid excessive heating, information should find application in tire design to avoid failures due to overheating. Figures 3; tables 1; references 3 (Russian).

Bismaleimide-Promoted Adhesion of EP and EPB Rubber to Lavsan

917M0127E Moscow KAUCHUK I REZINA in Russian No 2, Feb 91 pp 32-33

[Article by N. N. Galanicheva, V. A. Glagolev, L. R. Lyusova and V. F. Ionova]

UDC 667.866:678.4:536.61

[Abstract] An analysis was conducted on the adhesiveness of ethylene-propylene (EP) and EP-butyl or - isobutylene (EPB) rubber to lavsan (Soviet Dacron) in relation to curing by peroximon F and incorporation of N,N'-(phenylene-1,3)bismaleimide (maleimide F). Maximum adhesiveness (1.8 kN/M) of EP rubber to lavsan was obtained with a composition consisting of 4 parts by wt. of peroximon F, 5 zinc oxide, 2 sulfur and 3.5 maleimide F in 100 parts by wt. of EP. In the absence of maleimide F adhesivess was $<$ 0.4 kN/M. Maximum adhesiveness of EPB approached 3.5 kN/M under the

following conditions (by wt.): 5 zinc oxide, 3 sulfena-mide C, 2 sulfur and 3 maleimide F per 100 EBP. Accordingly, maleimide F was shown to be effective in enhancing adhesion of EB and EBP rubbers to lavsan when compounded in the proper proportions. Figures 1; references 4: 2 Russian, 2 Western.

Effects of Zinc Oxide on Synthesis of Rubber Intended for Food Contact

917M0127F Moscow KAUCHUK I REZINA in Russian No 2, Feb 91 pp 34-35

[Article by M. L. Uralskiy, Yu. G. Chikishev, E. Z. Olpinskaya and B. V. Filippovich]

UDC 678.4.033..3;678.04.01

[Abstract] An analysis was conducted on factors affecting Zn migration from nitrile rubber intended for food contact. Studies on water and acid extracts of nitrile rubber compounded with different concentrations of ZnO and powdered silica gel showed that the latter exerted a two-fold beneficial effect. In addition to accelerating curing, silica gel was also shown to trap and bind ZnO and thereby prevent the leaching of zinc from nitrile rubber. Use of silica gel was particularly important in nitrile rubber containing $> 0.4\%$ ZnO. Tables 2; references 2 (Russian).

Radiochemical Removal of Nitrogen and Sulfur Oxides From Gas Effluents of Thermal Power Stations

[Article by G.Ya. Gerasimov, T.S. Gerasimova, I.P. Tokmacheva, S.A. Fadeyev, and M.V. Faminskaya, Scientific Research Energy Institute imeni G.M. Krzhizhanovskiy]

UDC 541.15:543.422

[Abstract] Kinetic studies were conducted on the chemical processess involved in the removal of nitrogen and sulfur oxides from gas effluents of thermal power stations by irradiation of the gases with fast electrons. The essence of the process, developed in Japan in the seventies, rests on the generation of atoms and radicals from N_2, O_2, CO_2, and H_2O, which react with NO and SO_2 to form nitric and sulfuric acid vapors. The addition of ammonia transforms the acids to the corresponding solid ammonium salts, which lend themselves to removal by dust collectors. The entire process can be described by nonlinear first-order differential equations and allows a prediction of results based on temperature and radiation dose. Figures 4; tables 1; references 13: 2 Russian, 11 Western.

Paramagnetic Sodium Ion Clusters in Irradiated NaA, NaX, and NaY Zeolites

[Article by G.A. Kuranova, Physicochemical Scientific Research Institute imeni L.Ya. Karpov]

UDC 541.15:549.67-114:543.422.27

[Abstract] In vacuo dehydrated NaA, NaX, and NaY zeolites subjected to gamma irradiation (NaA, 50 kGy; NaX and NaY, 85 kGy) at 77 K were studied for paramagnetic sodium ion clusters by EPR spectroscopy. Analysis of the EPR spectra demonstrated, in addition to hole defects, 7-line (NaA) and 13-line (NaY, NaX) spectra due to, respectively, Na_2^+(NaA) and Na_4^{3+}(NaX and NaY) paramagnetic ion clusters. The formation of these clusters was attributed to free electron capture by groups of sodium ions. Na_2^+ clusters in NaA suggests that clusters with more than two Na ions are unstable or that the Na_2^+ clusters are located outside the cubic octahedral cells. Figures 1; tables 1; references 20: 4 Russian, 16 Western.

Transit of Fast Electrons in Lamellar Targets

[Article by I.R. Yentinzon, A.S. Kutsenko, and A.P. Meleshevich, Institute of Physical Chemistry imeni L.V. Pisarzhevskiy, Ukrainian SSR Academy of Sciences]

UDC54.185+541.15

[Abstract] Studies were conducted on the transition of fast electrons in 30- and 90-μm-thick cellulose diacetate films on various solid substrates with different atomic numbers (Z). The targets were irradiated by a sinusoidal electron beam produced by a UE-0.4M accelerator with a maximum energy of 0.35 MeV. The results demonstrated that the absorbed dose in the organic layers increased with an increase in the Z value of the solid support to ca. Z = 53, reaching a plateau with further increases in Z. This relationship between the dose and Z was explained on the basis of Rutherford's postulated elastic electron scatter on impact with a nucleus, which is equal to Z^2, and loss of energy by the scattered electrons due to inelastic collisions within the support substrate. Additional factors affecting the absorbed dose include the thickness of the air layer over the organic coat and the energy level of the fast electrons. For example, in the case of 1-MeV electrons the dose-Z relationships reached a plateau at Z = $\leq$ 35. Figures 3; references 20: 12 Russian, 8 Western.

Gamma Ray-Induced Radiochemical Transformations in Aminoimide Foam Plastic

[Article by V.V. Lyashevich, N.I. Trofimova, and V.G. Yurchenko]

UDC 541.15:678.84

[Abstract] Physicochemical studies on polyaminoamide foam plastic subjected to gamma irradiation demonstrated its relative radioresistance. The studies were performed with foam plastic synthesized from 4,4'-diaminodiphenylmethane and N,N'-(4,4'-diphenylmethane)-bis-maleinimide in a 1:2 ratio, irradiated at 40° with Co-60 γ-rays in doses reaching 100 MGy (2.7 Gy/sec). Thermomechanical analysis, determinations of volatile products, and IR spectroscopy showed that the radiation-induced oxidation processes in the plastic included hetero- and homolytic disruption of polymeric chains. Nevertheless, the compression strength of the foam plastic was reduced from an initial value of 6.2 to 5.3 MPa in the extreme case. This indicates that practical applications of the polyaminoamide foam were not seriously affected. Figures 4; tables 1; references 9: 8 Russian, 1 Western.

Conductometric Studies on Track Structure of Charged Ions in Polymers

[Article by P.Yu. Apel]

UDC 541.15

[Abstract] Conductometric studies on tracks formed by accelerated Xe and Kr ions in polyethyleneterephthalate, polycarbonate, polyarylate, and polypropylene showed that they resembled a pair of coaxial cylinders consisting of a inner core and an outer envelope. The core represents an area of matrix destruction with the generation of ions, including "hot" and thermal hydrogen atoms that react with the polymer to form an assortment of radicals. Radial diffusion of these reactive elements to a distance of 30-50 nm and reaction with the matrix are responsible for the cross-linking in the envelope. In addition, envelope phenomena due to delta electron effects are predicted, and the contribution of each factor determines the final extent of cross-linking. Figures 4; references 20: 7 Russian, 13 Western.

Radiolytic Transformations in Aqueous Serum Albumin Solutions

[Article by N.A. Vysotskaya and V.M. Russakovskiy, Institute of Physical Chemistry imeni L. V. Pisarzhevskiy, Ukrainian SSR Academy of Sciences]

UDC 541.15

[Abstract] Physicochemical studies were conducted on human and bovine serum albumin solutions subjected to Co-60 gamma irradiation (to 10 kGy, 15-30 Gy/sec) at room temperature to determine radiolytic products responsible for conformational changes. The data showed that 3-5 kGy is sufficient for most of the changes in the supramolecular structure of albumin. The findings were consistent with a process involving rupture of peptide chains and intermolecular cross-linking. Hydrated electrons and hydrogen atoms were primarily responsible for the former process, whereas hydroxyl radicals were primarily responsible for the latter. Finally, the most profound conformational changes occur at the isolectric point of albumin, which corresponds to its most compact state. figures 2; tables 1; references 4 (Russian).

Calculation of the Effect of Gas Phase Inhibition on the Structure and Extinguishing of Hydrogen- and Methane-Air Extended Flames

[Article by V.N. Lebedev]

UDC 536.46

[Abstract] The effect of hydrodynamic deformation on the process of gas phase inhibition of frontal combustion was studied by using a model of a planar, homogeneous laminar flame, with one counterflow of the burning mixture and/or the products of its adiabatic combustion. The first case is a symmetrical double flame, the second is a single-front flame. In an extension of the previous work by the author, the kinetics of inhibition were found to reflect a strong dependence of normal flame characteristics on small (1-3%) additions of hydrogen bromide to the initial mixture. At flow rate gradients above the critical value, an unstable transition to a simpler heat mass transfer regimen occurs, with a very weak chemical reaction. Significant hysteresis in the flow rate gradient was found. Calculations also demonstrated strong sensitivity to a change in inhibitor concentrations. Figures 4; references 4: Russian.

UDC 614.841.12

The Effect of Elevated Pressure and Temperature on the Combustion of Steam and Gas Mixtures

[Article by A.Ya. Korolchenko, S.G. Tsarichenko, Yu.N. Shebeko, and O.Ya. Yeremenko]

[Abstract] The effect of pressure on the upper concentration limit of flame propagation in hydrocarbon-hydrogen mixtures and the normal combustion rate of hydrogen-air-steam mixtures at elevated temperatures were investigated. The concentration limit of flame propagation was found to increase with an elevation in the initial pressure in CH_4-air, C_3H_8-air and C_3H_8-H_2-air mixtures. More complete combustion was seen in a 100-mm-diameter vertical vessel than in a 30-mm vessel. The expression $C = C_0 + 3.5 \ln (P/P_0)$ was developed to describe the results found. In this expression C and C_0 are the final and initial concentration limits of flame propagation, while P and P_0 are the final and initial pressures. For hydrogen-air mixtures in the absence of steam, the normal combustion rate increased with increasing pressure. However, the addition of as little as 5%(vol) steam caused the combustion rate to decrease with increasing pressure. This effect was more pronounced at 30%(vol) steam. Experiments were conducted at 473-673 K. Figures 2; references 13: 7 Russian, 6 Western.

Combustion Limits of Hydrocarbons at Low Pressure and Temperature

[Article by S.G. Alekseyev, V.K. Manzhos, and A.L. Dmitriyev]

UDC 536.468:662.69

[Abstract] The concentration limits of the combustion of oxygen- methane, oxygen-methane-nitrogen, oxygen-propane, and air-propane mixtures were determined at pressures below atmospheric. Low temperatures were also studied for oxygen-methane and oxygen-propane mixtures. Lowering the temperature to 243 K increased the lower limit from 5.1%(vol) to 6%(vol) and the upper limit from 57%(vol) to 60%(vol). Lower pressure resulted in a decrease in the limits of combustion, particularly the lower limit. Introduction of large quantities of nitrogen into a methane-oxygen mixture led to a sharp decrease in the combustion range toward the methane-rich direction and a simultaneous increase in the pressure limits of combustion. Lowering the temperature of a propane-oxygen mixture containing small amounts of carbon dioxide, argon, nitrogen, and water vapor led to an expansion of the lower concentration limit of combustion with an increase in the minimum combustion pressure. The pressure limit was higher for propane-air mixtures than for propane-oxygen. For propane-air mixtures at 293K two pressure concentration limit minima were observed, one at the stoichiometric concentration and the other at 8.25%(vol) propane. The concentration limits also depended on ignition energy. Figures 4; references 3: Russian.

The Role of Scale-Up Effect in Flame Acceleration by Barriers

[Article by V.A. Gorev and V.N. Fedotov]

UDC 536.46-537.222.2

[Abstract] The effect of scale-up on flame acceleration was studied under geometrically similar conditions with identical burning mixtures by using a cubic network of rods as a barrier. The large-scale apparatus used was in the form of an octagonal prism and was of the authors' design. A stoichiometric propane-air mixture was used to form a semispherical flame. Geometrically similar obstacles were found to accelerate combustion differently depending on the scale of the obstacle. Larger obstacles accelerated combustion more strongly. An expression was derived for the coefficient of combustion intensification in terms of barrier diameter, flame area, and combustion rate. The expression is intended for cases where the distance between barrier elements is not more than ten times an element's diameter. The value of

the empirical factor included in the expression was determined for various sets of conditions. Figures 1; references 10: 8 Russian, 2 Western.

A Model of Aluminum Particle Combustion Including Kinetic Factors

[Article by I.M. Kiryanov, V.I. Malinin, Ye.I. Iotelnik-ova, and A.V. Sukhov]

UDC 536.46

[Abstract] A model is proposed for the combustion of small aluminum particles that involves the melting of aluminum oxide at the start of combustion to form spherical droplets on the surface of the particles. It is proposed that oxidation of aluminum occurs directly on the outer surface of the oxide, as well as in the space surrounding the particles. This assumption permits an explanation of the observed small change in the obstacle. Larger obstacles accelerated combustion more strongly. An expression was derived for the coefficient of combustion intensification in terms of barrier diameter, flame area, and combustion rate. The expression is intended for cases where the distance between barrier elements is not more than ten times an element's diameter. The value of the empirical factor included in the expression was determined for various sets of conditions. Figures 1; references 10: 8 Russian, 2 Western.

Propagation of a Laminar Flame in Mono- and Polydisperse Aerosuspensions

[Article by D.A. Yagodnikov, A.V. Voronetskiy, A.V. Sukhov, and D.G. Pavlov]

UDC 536.46;541.126

[Abstract] A mathematical model was used to investigate the propagation of the laminar flame front in a polydisperse suspension of fuel particles in gas. The probability density distributions of temperature and particle diameter had the greatest effect on flame and combustion characteristics. A unidimensional spherical coordinate system was used, and a coefficient of conditional migration was defined as proportional to the relaxation time and mean reactive speed of the particles. A system of ten equations was developed and tested with polydisperse aluminum particles as an example. Two maxima in the probability density distributions were observed. Deeper into the flame, burnout of smaller particles predominated. Even if the aerosol began combustion in a monodisperse state, it was calculated to become polydisperse due to burnout and reactive migration. The flame front propagation rate increased with decreasing excess air. The contribution of radiative heat flow did not exceed

about 10% of the total heat evolution of the system. The rate of flame front propagation was greater in a polydisperse system than in a monodisperse one. The results of the calculations agree with the experimental observations of other authors. The flame front propagation rate also increased with increasing diffusion coefficients. The model developed makes it possible to investigate turbulent combustion. Figures 3; references 6: 5 Russian, 1 Western.

The Interaction of Carbon Particles Burning at a High Temperature

[Article by V.A. Nastasyuk and M.N. Chesnokov]

UDC 536.46

[Abstract] The Labowski method, involving transformation of transfer equations into Laplace equations and solution of the equations by using the mirror image method, was applied to the combustion of carbon particles at high temperatures not exceeding 2,500 K. The equations describing mass and temperature distribution were transformed. Simultaneous solution of the two resulting equations gave a unique value of temperature and surface mass fraction for each particle. Summation and integration of these values resulted in a formula for the average macroscopic combustion rate of the aerosol in terms of particle concentration. As a result, the character of the influence of the carbon fuel particles on each other was clarified. References 7: 2 Russian, 5 Western.

Calculation of Heat Radiation From a Sooty Flame in an Axisymmetric Combustion Chamber

[Article by S.A. Volkov]

UDC 536.46

[Abstract] This article presents a method for calculating heat radiation flows from an axisymmetric sooty flame when the temperature distribution and soot concentration are known. The combustion chamber was represented as one or two coaxial cylinders with diffusely radiating and reflecting walls. Solution of the equation describing the spectral intensity distribution equation and subsequent integration after transformation by using the axis of symmetry of the combustion chamber were performed. Numerical integration over the flow radius and angle was based on use of the Gauss-Legendre quadratic formula. The method was also used to calculate the integral semispherical flow from a sooty flame falling on the walls of a tubular combustion chamber of a gas turbine engine. The results obtained agree with

results obtained by the spherical harmonics method. Figures 3; references 6: 5 Russian, 1 Western.

Model of Ignition of Polymeric Materials by Laser Radiation

[Article by S.G. Bychkov and G.I. Ksandopulo]

UDC 536.46:621.375

[Abstract] A model is proposed for the gas phase combustion of polymeric materials that gives consideration to the physical nature of the heat flow source. The time for formation of the necessary temperature gradient at the surface depends on the nature of the heat source. Formation of the heated layer solely from background heat transfer represents one extreme, while energy evolution due to absorption of electromagnetic radiation represents the other. Equations were derived for laser radiation in order to simplify evaluation of energy absorption. Analytical expressions were developed for the flame induction period, including both types of heat source. The gas-phase combustion channels will differ depending on the tendency of the polymer to coke formation. With high levels of coke formation, condensed pyrolysis products play an important role. For polymers exhibiting low levels of coke formation, the basic energy evolution zone may be found in the coagulate of gaseous pyrolysis products so that the flame foci are associated with various density fluctuations. Chain reaction-type mechanisms are very probable in this case. References 10: Russian.

Combustion of Dust Cloud Due to Heat Foci

[Article by R.S. Burkina]

UDC 536.46

[Abstract] The development of focal explosions in a gaseous medium containing solid burning particles was analyzed. The development of combustion foci was taken to be connected with abrupt temperature changes due to compression or movement of a dust cloud layer. The onset time of the heat foci was taken to be significantly less than the development time. Homogeneous particle distribution and a particle radius much smaller than the heat focus size were also assumed. The critical process was obtained from a system of equations describing temperature evolution, solution of which was accomplished by using the asymptotic decomposition fusion method. As a result, equations for ignition time and critical ignition time, in terms of the Frank-Kamenetskiy parameter, were obtained. The case in question differed from the homogeneous case in the

appearance of a factor in the Frank-Kamenetskiy parameter equation representing the intensity of heat transfer between gas and particles. Mass concentration was found to have no effect on the major term of the asymptotic decomposition. When experimental data for which the Frank-Kamenetskiy parameter was found to be 0.305 were used, a value of 0.435 resulted from the equations derived in this article. References 5: 4 Russian, 1 Western.

Nonstationary Effects on the Hydrodynamics and Intensification of Metallic Fuel Combustion

[Article by A.G. Yegorov, K.V. Migalin, G.I. Ovchinnikova, A.I. Samodurov, A.P. Shaykin, and S.Ya. Yagubyan]

UDC 662.612.1.001.2

[Abstract] The effect of a nonstationary regime on the hydrodynamics and intensification of the combustion of highly dispersed AMD-50 aluminum-magnesium alloy powder was studied by using sudden expansion and pulsed air jets. The alloy powder particle diameter was 10-12 μm. Changing air jet pulse frequency from 0 to 150 Hz increased the length of the recirculation zone by 20%, while further increases in frequency decreased the zone length. Above 200 Hz the scale of the flow vortex decreased. The pulsed air caused the temperature maximum isotherms to shift from the edges of the combustion chamber toward the middle. Temperature inhomogeneity decreased. The maximum temperature was greatest at 300 Hz. The results indicate that the pulsed air jets increased the size of the flame front surface and favored axial recirculation. Pulse frequency can be used to control the characteristics of the reversed-flow zone. Figures 3; references 7: 5 Russian, 2 Western.

Combustion of Finely Divided Aluminum Powder in a Stream of Air

[Article by A.G. Yegorov, K.V. Migalin, V.Ya. Niyazov, M.M. Rusakov, V.A. Sovetov, and A.P. Shaykin]

UDC 662.612.1.001

[Abstract] Ignition and flame stabilization were studied in the combustion of aluminum powder by using a tungsten, steel, or copper wire screen placed at one of eight positions in an axially symmetrical combustion chamber with electrical ignition and sudden expansion. Chamber dimensions permitted limited jet turbulence with stalled flow at the closed bottom. Particle diameter varied from 10 μm to 450 μm. Start-up limits and flame stabilization were measured at 288 K. Decreased fineness of fuel particles permitted combustion of richer

fuel-air mixtures. The maximum rate was achieved at a fuel-to-air ratio of 1.3. Increasing the ratio of chamber diameter to feed line diameter widened the stable combustion area. Increased turbulence increased the flame volume and completeness of combustion. The highest temperature measured in the combustion product jet was 3,573 K. The results demonstrate the stabilization of aluminum powder flames over a wide range of rates and compositions in a combustion chamber with sudden expansion. Figures 3; references 4: Russian.

Thermal Explosion Zones Elicited by Pulsed Radiation

[Article by O.B. Vorozhtsova]

UDC 534.222.2+536.46

[Abstract] The concept of thermal explosion foci was used to mathematically describe the combustion of transparent solid explosive substances caused by radiation. Assuming that the areas absorbing radiation are spherical and that thermokinetic constants do not change with time and neglecting thermal field interactions, a system of partial differential equations describing the thermal state of the absorbing particles and their surroundings was developed. In order to solve these equations, it was necessary to determine the critical explosion energy, the minimum energy needed to initiate a chain reaction. Using the asymptote method, expressions were obtained for the critical energy and time to development of an explosion in terms of pulse length, focus dimensions, and thermokinetic criteria. Several approximations were used to develop a formula for critical energy absorbed per unit particle volume. Results obtained with this formula for lead azide gave good agreement with iteration-interpolation results obtained from the initial partial differential equations. Critical energy was found to increase with total radiation time due to an increased role for heat dissipation. Figures 3; references 7: Russian.

The Characteristics of the Nonstationary Combustion of Mixed Solid Fuels When They Are Exposed to Laser Radiation

[Article by V.N. Simonenko, V.M. Fomenko, and A.G. Svit]

UDC 536.46

[Abstract] The concept of thermal explosion foci was used to mathematically describe the combustion of transparent solid explosive substances caused by radiation. Assuming that the areas absorbing radiation are spherical and that thermokinetic constants do not

change with time and neglecting thermal field interactions, a system of partial differential equations describing the thermal state of the absorbing particles and their surroundings was developed. In order to solve these equations, it was necessary to determine the critical explosion energy, the minimum energy needed to initiate chain reaction. Using the asymptote method, expressions were obtained for the critical energy and time to development of an explosion in terms of pulse length, focus dimensions and thermokinetic criteria. Several approximations were used to develop a formula for critical energy absorbed per unit of particle volume. Results obtained with this formula for lead azide were in good agreement with the iteration/interpolation between the combustion rate and the dimensionless resonance frequency and made it possible to extrapolate to higher pressures, which is useful for the evaluation of ballistic fuels. Figures 5; references 7: Russian.

Features of Temperature Distribution in Condensed Phase Reagents During Self-Oscillating Combustion

[Article by V.I. Zemskikh, V.M. Puchkov, and A.V. Timchenko]

UDC 536.46

[Abstract] Numerical experiments were used to study the temperature profiles that arise during self-oscillating combustion. Plots of the temperature profile at various points of time exhibited no maxima, minima, or inflection points. Plots of a variable constructed to represent the reading that would be obtained from an ideal thermocouple at a fixed distance from the surface exhibited inflection points. Correlation coefficients for combustion rates calculated from the tangents of the latter curves, when plotted against actual data, ranged from 0.3 to 0.7. The results indicate that this correlation is not strong. One may conclude that identification of self-oscillating combustion via registration of temperature in the condensed phase requires rigorous formulation of the opposite question. Figures 4; references 4: Russian.

Modeling the Coke Formation Process in the Combustion of Polymeric Materials

[Article by V.I. Kodolov and A.M. Lipanov]

UDC 536.46

[Abstract] Coke formation as a result of the combustion of polymeric materials was divided into seven classes: 1) the ideal case, in which there are practically no pores in the carbon covering or heat flow from the surface, with maximal heat conductivity; 2) the case of the formation

of many small pores in the coke covering; 3) the case of layered coke covering, with the structure of the bottom layer a result of bubble formation; 4) the case of large pores in the coke, with a coke density similar to that of the starting material; 5) the case of amorphous porous coke containing a significant percentage of large pores and craters; 6) the case of amorphous porous coke containing gaseous bubbles; and 7) the case of nonporous coke film. A mathematical model was constructed for both "dry" and "wet" surfaces, including mesotropic conversions in polymer composition. This resulted in a partial differential equation of heat conduction. The polymeric materials have active components that form either gaseous and solid products, or gaseous, liquid, and solid products on combustion. The materials also have passive components that remain mostly in the coke formed. In order to facilitate solution of the kinetic equations and decrease error, it was assumed that weak chemical bonds are destroyed first, forming more bonds that are more stable to oxidation or thermal oxidation. Use of the model for pyrolysis of polyacrylonitrile and cellulose gave calculations for coke formation in good agreement with experimental observations. References 3: Russian.

Features of Carbidizing Treatment of Spongy Titanium During Its Combustion in the Presence of Halogen-Containing Additives

917M0058Q Moscow KHIMICHESKAYA FIZIKA in Russian Vol 9 No 12, Dec 90 pp 1682-1685

[Article by V.N. Nikogosov, G.A. Nersisyan, S.L. Kharatyan, and A.G. Merzhanov]

UDC 536.46.546.821

[Abstract] The combustion of spongy titanium with carbon black in the presence of TF-4 fluoroplastic or hexachlorobenzene was investigated for the purpose of devising a procedure for synthesizing stoichiometric titanium carbide. Combustion was conducted in a bomb with constant pressure and an argon atmosphere. The temperature and rate of combustion were found to reach maxima at lower C:Ti ratios than those observed with powdered titanium. When one tenth or one twentieth of the amount of carbon was replaced with fluoroplastic, there was no effect on temperature or the rate of combustion, but less incomplete combustion was seen due to a decrease in kinetic and structural hindrances. The titanium carbide produced exhibited a well-formed cubic structure. Crystal dimensions were as large as 0.1 mm. Cubic TiF_3 crystals were seen in the core of the product. Increasing the amount of fluoroplastic increased the combustion temperature. For hexachlorobenzene, the maximum combustion temperature was noted at 5 mol.%. When the fluoroplastic level was 1-2 mol.% and the carbon level was 38-39 mol.%, the combustion temperature was 1900-2000 , and the combustion propagation rate was 0.1-0.12 cm/sec. These conditions gave a product with about 20% total carbon, of

which 0.5-1% was free carbon. The results indicate that incomplete combustion was reduced to a 3-5% level. Figures 4; references 4: Russian.

Structural Rules for the Formation of Diamond and Boron Nitride in Shock Waves

917M0058R Moscow KHIMICHESKAYA FIZIKA in Russian Vol 9 No 12, Dec 90 pp 1686-1688

[Article by N.I. Borimchuk, A.V. Kurdyumov, and V.V. Yarosh]

UDC 539.893:548.33

[Abstract] A method was developed at the Institute of Applied Minerology of the UkSSR Academy of Sciences for shock compression; this method permits heating to high temperatures during compression and sufficiently rapid cooling on discharge. Using this method made it possible to significantly decrease the synthesis pressure and gave yields of diamond from graphite to 60%, diamond from carbon black to 90%, and sphalerite cubic boron nitride to 70%. When compressing highly crystalline graphite with a high degree of ternary ordering, the graphite-to-diamond conversion proceeded by the martensitic mechanism, with the formation of an lonsdalite intermediate. The final product contained no more than 40-45% lonsdalite, in contrast to product obtained by static compression, which may contain as much as 90% lonsdalite. The amount of lonsdalite obtained decreased with increasing temperature. Smaller lonsdalite crystals were obtained by shock compression than those reported for static compression. Shock compression of carbon black did not produce lonsdalite since the martensitic mechanism is not possible. Conversion of turbostratic boron nitride to sphaleritic required temperatures around 3,500°C and rapid quenching. Very small crystals of diamond from carbon black and sphaleritic boron nitride were produced. The data demonstrate that varying the temperature of shock compression and improving the structure of the starting material can change the mechanism of carbon and boron nitride phase transformation, as well as the phase composition and structure of the products. References 6: 4 Russian, 2 Western.

Limits on the Rate of Combustion Wave Propagation in Solid Residues of Polymer-Containing Material

917M0058S Moscow KHIMICHESKAYA FIZIKA in Russian Vol 9 No 12, Dec 90 pp 1693-1696

[Article by S.Ye. Selivanov and A.A. Shiyan]

UDC 536.46

[Abstract] The possible limits on the rate of propagation of the solid-residue afterburning wave in fiberglass combustion were analyzed. The fiberglass fibers were oriented in the same direction as the air flow. The wave

propagation rate and front temperature were essentially constant during combustion. The differential equations describing heat conduction and change in the quantity of burning solid residue were used to construct a mathematical model of the process. Linearization led to a dispersion equation, solution of which gave the minimal and maximal propagation rates. The minimum propagation rate was $\pi a/l$, where a is the temperature conduction coefficient of the fiberglass and 1 is the width of the afterburning wave. References 7: Russian.

Foreign Broadcast Information Service (FBIS) and Joint Publications Research Service (JPRS) publications contain political, military, economic, environmental, and sociological news, commentary, and other information, as well as scientific and technical data and reports. All information has been obtained from foreign radio and television broadcasts, news agency transmissions, newspapers, books, and periodicals. Items generally are processed from the first or best available sources. It should not be inferred that they have been disseminated only in the medium, in the language, or to the area indicated. Items from foreign language sources are translated; those from English-language sources are transcribed. Except for excluding certain diacritics, FBIS renders personal and place-names in accordance with the romanization systems approved for U.S. Government publications by the U.S. Board of Geographic Names.

Headlines, editorial reports, and material enclosed in brackets [ ] are supplied by FBIS/JPRS. Processing indicators such as [Text] or [Excerpts] in the first line of each item indicate how the information was processed from the original. Unfamiliar names rendered phonetically are enclosed in parentheses. Words or names preceded by a question mark and enclosed in parentheses were not clear from the original source but have been supplied as appropriate to the context. Other unattributed parenthetical notes within the body of an item originate with the source. Times within items are as given by the source. Passages in boldface or italics are as published.

SUBSCRIPTION/PROCUREMENT INFORMATION

The FBIS DAILY REPORT contains current news and information and is published Monday through Friday in eight volumes: China, East Europe, Soviet Union, East Asia, Near East & South Asia, Sub-Saharan Africa, Latin America, and West Europe. Supplements to the DAILY REPORTs may also be available periodically and will be distributed to regular DAILY REPORT subscribers. JPRS publications, which include approximately 50 regional, worldwide, and topical reports, generally contain less time-sensitive information and are published periodically.

Current DAILY REPORTs and JPRS publications are listed in *Government Reports Announcements* issued semimonthly by the National Technical Information Service (NTIS), 5285 Port Royal Road, Springfield, Virginia 22161 and the *Monthly Catalog of U.S. Government Publications* issued by the Superintendent of Documents, U.S. Government Printing Office, Washington, D.C. 20402.

The public may subscribe to either hardcover or microfiche versions of the DAILY REPORTs and JPRS publications through NTIS at the above address or by calling (703) 487-4630. Subscription rates will be provided by NTIS upon request. Subscriptions are available outside the United States from NTIS or appointed foreign dealers. New subscribers should expect a 30-day delay in receipt of the first issue.

U.S. Government offices may obtain subscriptions to the DAILY REPORTs or JPRS publications (hardcover or microfiche) at no charge through their sponsoring organizations. For additional information or assistance, call FBIS, (202) 338-6735,or write to P.O. Box 2604, Washington, D.C. 20013. Department of Defense consumers are required to submit requests through appropriate command validation channels to DIA, RTS-2C, Washington, D.C. 20301. (Telephone: (202) 373-3771, Autovon: 243-3771.)

Back issues or single copies of the DAILY REPORTs and JPRS publications are not available. Both the DAILY REPORTs and the JPRS publications are on file for public reference at the Library of Congress and at many Federal Depository Libraries. Reference copies may also be seen at many public and university libraries throughout the United States.